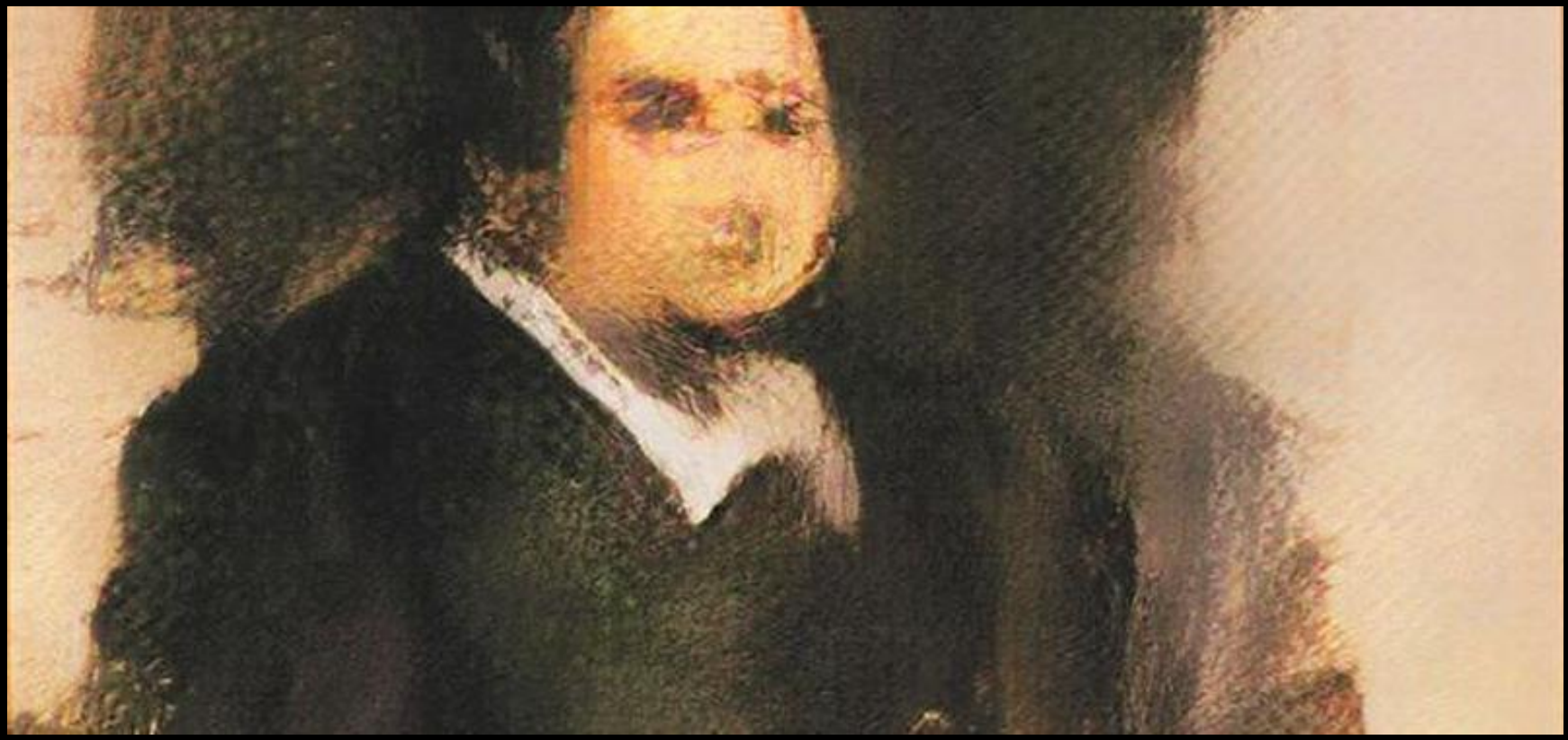

# Adversarial Examples, VAEs and GANs
# CS 410/510: CV & DL

# First…A Message from Mark

# Outline

- Adversarial Examples
- Applications of GANs/VAEs
- VAEs
- GANs
- *GAMEGAN*
- Graph Neural Networks

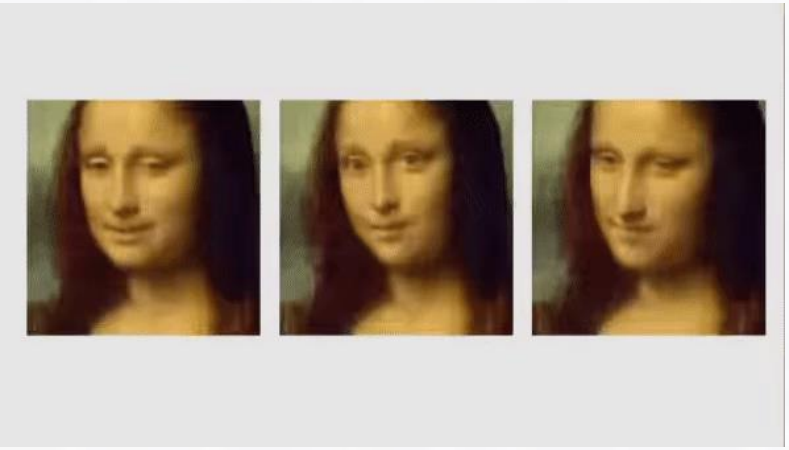

# Adversarial Examples

• In 2015, Ian Goodfellow et al., published a landmark paper "Explaining and Harnessing Adversarial Examples."*

EXPLAINING AND HARNESSING ADVERSARIAL EXAMPLES

**Ian J. Goodfellow, Jonathon Shlens & Christian Szegedy**
Google Inc., Mountain View, CA
{goodfellow,shlens,szegedy}@google.com

• This research is remarkable in the history of ML for at least two dominant reasons:

(1) It <u>demonstrated the general brittleness of deep models</u> (and data-driven ML workflows more generally); this work proved the existence of adversarial examples to be a *feature of DNNs* and not a bug.

*https://arxiv.org/pdf/1412.6572.pdf

# Adversarial Examples

• In 2015, Ian Goodfellow et al., published a landmark paper "Explaining and Harnessing Adversarial Examples."*

EXPLAINING AND HARNESSING ADVERSARIAL EXAMPLES

**Ian J. Goodfellow, Jonathon Shlens & Christian Szegedy**
Google Inc., Mountain View, CA
{goodfellow,shlens,szegedy}@google.com

• This research is remarkable in the history of ML for at least two dominant reasons:

(1) It <u>demonstrated the general brittleness of deep models</u> (and data-driven ML workflows more generally); this work proved the existence of adversarial examples to be a *feature of DNNs* and not a bug.

Despite their recent "superhuman" successes, this research spawned a renewed interest in improving the robustness of deep models, debiasing these models, and enhancing their interpretability – all essential steps toward realizing the broad adoption of DL-based algorithms in commercial products.

(2) It pointed toward a <u>methodology to generate adversarial examples</u>, and bears close conceptual ties with GANS, which we discuss later.

*https://arxiv.org/pdf/1412.6572.pdf

# Adversarial Examples

• In fact, adversarial DL examples were described prior to the Goodfellow paper of 2015, including in a well-known paper by Szegedy** – a co-author of the Goodfellow paper – in the year prior.

• It was previously conjectured that DNNs were susceptible to adversarial examples – but early research attributed the existence of these attacks to the non-linear characteristics of DNNs. The Goodfellow paper argued, conversely, that the linear nature of DNNs – the very thing that made them easy to train, makes them susceptible to such examples.

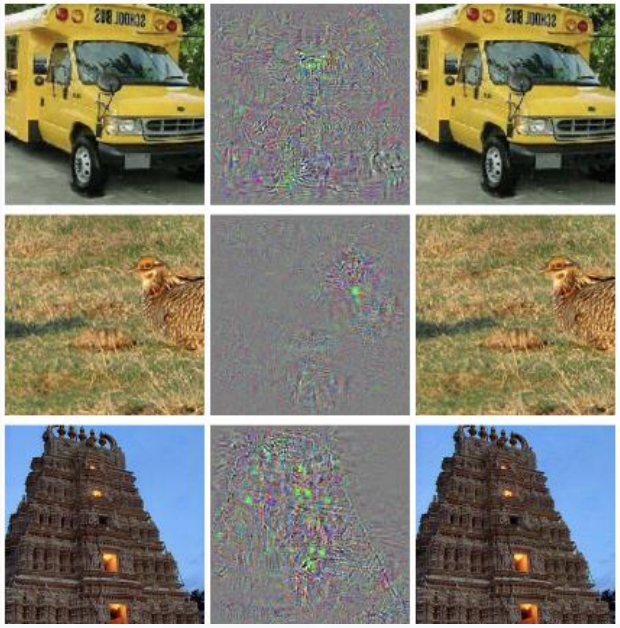

* https://arxiv.org/pdf/1312.6199.pdf

# Adversarial Examples

• The argument in the paper is as follows: In many problems, the precision of an individual input feature is limited; for instance, with 8-bit images, we discard any visual information falling below the 1/255 dynamic pixel intensity range.

Define a perturbed image as: $\tilde{\boldsymbol{x}} = \boldsymbol{x} + \boldsymbol{\eta}$, where $\boldsymbol{x}$ denotes the original image and $\boldsymbol{\eta}$ the perturbation, where $\|\boldsymbol{\eta}\|_\infty < \varepsilon$, which is to say that all the features of $\boldsymbol{\eta}$ are below the $\varepsilon$-precision value.

• Because $\|\boldsymbol{\eta}\|_\infty$ does not grow with the dimensionality of the problem, this means that we can make many infinitesimal changes to the input that add up to one large change to the output. Which is to say that small perturbations to each pixel can result in a vastly different model prediction.

# Adversarial Examples

• Indeed, the researchers demonstrate that this phenomenon generalizes across models of vastly different complexity – from basic logistic regression models to DNNs.

• They introduce a methodology, termed the "**fast gradient sign method**" (FGSM). Using gradient-descent, they solve for a max-norm (i.e., $\|\boldsymbol{\eta}\|_\infty < \varepsilon$) constrained perturbation:

$$\boxed{\boldsymbol{\eta} = \varepsilon \cdot sign(\nabla J(\boldsymbol{\theta}, \mathbf{x}, y))}$$

where sign(·) is the **signum function** $\boldsymbol{\Theta}$ denotes the model parameters, $\boldsymbol{x}$ is the input the model and $\boldsymbol{y}$ is the target associated with $\boldsymbol{x}, J(\boldsymbol{\Theta}, x, y)$ is the cost function used to train the NN, and the final perturbed image is defined by: $\tilde{\boldsymbol{x}} = \boldsymbol{x} + \boldsymbol{\eta}$.

(*) Notice that from this definition, $\boldsymbol{\eta}$ is a vector pointing in the direction of maximum changing (with respect to the objective function $J$, where the condition $\|\boldsymbol{\eta}\|_\infty < \varepsilon$ is maintained.

# Adversarial Examples

$$\boldsymbol{\eta} = \varepsilon \cdot sign(\nabla J(\boldsymbol{\theta}, \mathbf{x}, y))$$

where sign(·) is the signum function, $\boldsymbol{\Theta}$ denotes the model parameters, $\boldsymbol{x}$ is the input the model and $\boldsymbol{y}$ is the target associated with $\boldsymbol{x}, J(\boldsymbol{\Theta}, x, y)$ is the cost function used to train the NN, and the final perturbed image is defined by: $\tilde{\boldsymbol{x}} = \boldsymbol{x} + \boldsymbol{\eta}$.

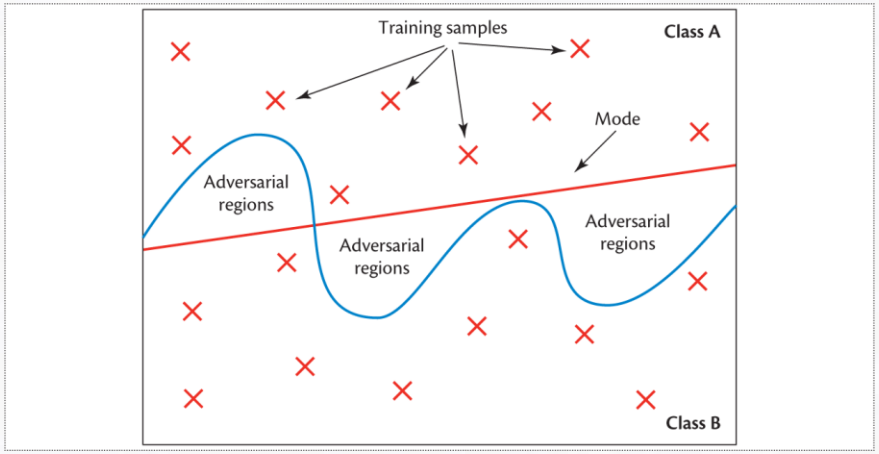


**In summary**: We leverage SGD to solve for the perturbation satisfying $\|\boldsymbol{\eta}\|_\infty < \varepsilon$ (so it is bounded, enforcing the total perturbation to be small); gradient steps are made in the direction of *maximum ascent*, so that we move "away" from a correct classification of the image.

• Notice that FGSM implicitly assumes that when crafting an adversarial example, one has "full access" to the NN training cost function $J(\boldsymbol{\Theta}, x, y)$. In a subsequent paper** (also co-authored by Goodfellow), the researchers demonstrate that "black box" (i.e., bereft of access to $J(\boldsymbol{\Theta}, x, y)$) adversarial attacks are also possible.

**https://arxiv.org/pdf/1602.02697.pdf

# Adversarial Examples

• Using FGSM, the authors cause a shallow softmax classifier to have an error rate of 99.9% on MNIST (with an average confidence of 79.3%), and a NN with 87.15% error rate on CIFAR-10.

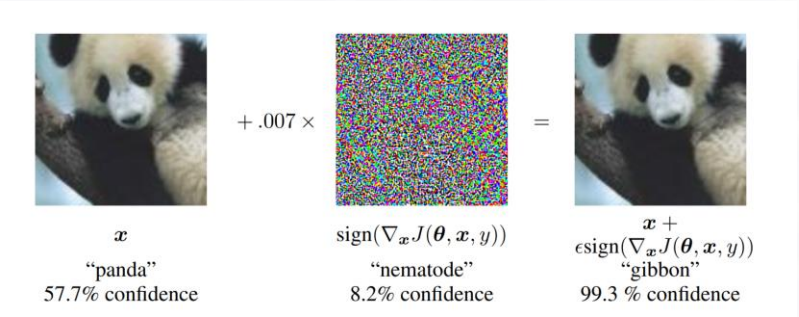

# Adversarial Examples

• Using FGSM, the authors cause a shallow softmax classifier to have an error rate of 99.9% on MNIST (with an average confidence of 79.3%), and a NN with 87.15% error rate on CIFAR-10.

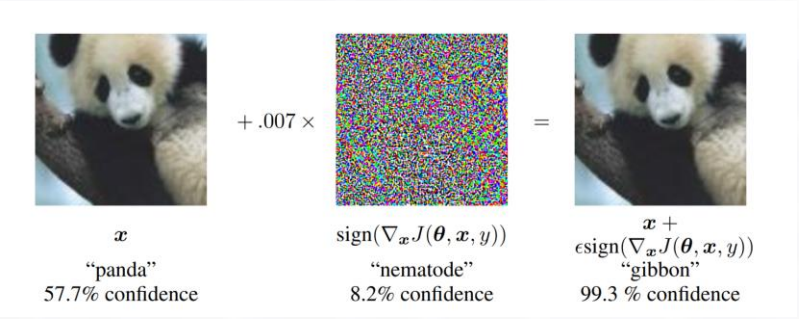


• Since the initial publication of this research, adversarial examples have been elicited and studied in a wide variety of domains (beyond images), including **audio applications***, **identity "dodging"****, and (not least of all), **adversarial training***** (where a model is intentionally trained on adversarial examples) to improved robustness.

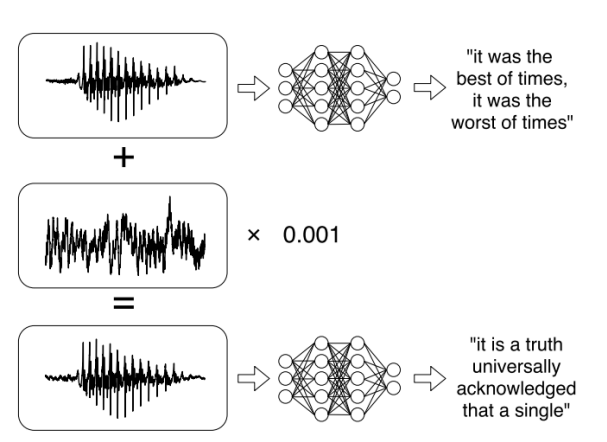


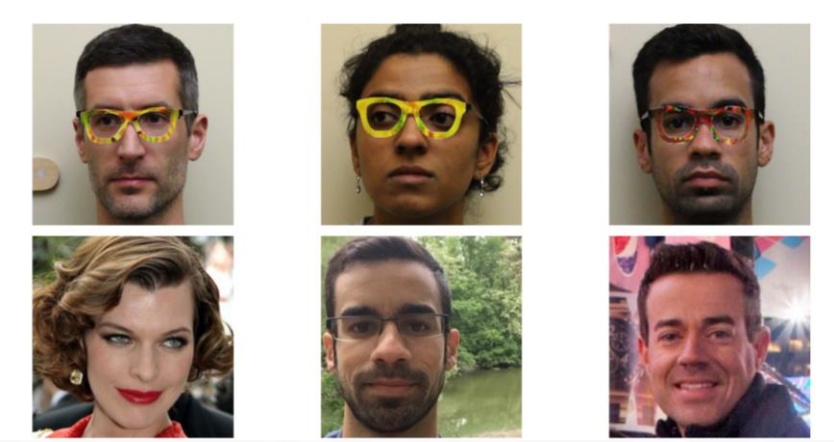

* https://arxiv.org/pdf/1801.01944.pdf
**https://arxiv.org/pdf/1801.00349.pdf
***https://papers.nips.cc/paper/2019/file/7503cfacd12053d309b6bed5c89de212-Paper.pdf

# GAN Applications

Thispersondoesnotexist.com

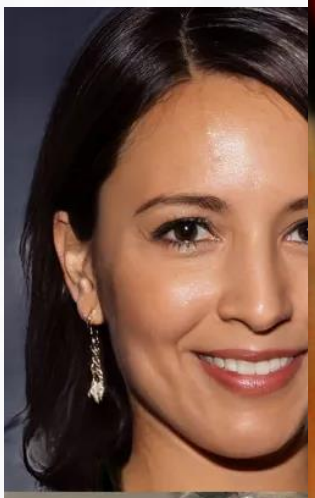

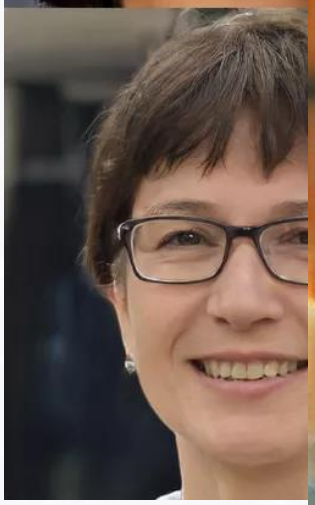

Thispersondoes

Sometimes it FAILS!

# GAN Applications: Google DeepDream

*Technically not using a GAN, bust still fundamentally uses a CNN as a generative model.

https://www.youtube.com/watch?v=sh-MQboWJug

# GAN Applications: Image/Video Upsampling

**Photo-Realistic Single Image Super-Resolution Using a Generative Adversarial Network**

Christian Ledig, Lucas Theis, Ferenc Huszár, Jose Caballero, Andrew Cunningham, Alejandro Acosta, Andrew Aitken, Alykhan Tejani, Johannes Totz, Zehan Wang, Wenzhe Shi
Twitter
{cledig,ltheis,fhuszar,jcaballero,aacostadiaz,aaitken,atejani,jtotz,zehanw,wshi}@twitter.com

**Abstract**

*Despite the breakthroughs in accuracy and speed of single image super-resolution using faster and deeper convolutional neural networks, one central problem remains largely unsolved: how do we recover the finer texture details when we super-resolve at large upscaling factors? The behavior of optimization-based super-resolution methods is principally driven by the choice of the objective function. Recent work has largely focused on minimizing the mean squared reconstruction error. The resulting estimates have high peak signal-to-noise ratios, but they are often lacking high-frequency details and are perceptually unsatisfying in the sense that they fail to match the fidelity expected at the higher resolution. In this paper, we present SRGAN, a generative adversarial network (GAN) for image super-resolution (SR). To our knowledge, it is the first framework capable of inferring photo-realistic natural images for 4× upscaling factors. To achieve this, we propose a perceptual loss function which consists of an adversarial loss and a content loss. The adversarial loss pushes our solution to the natural image manifold using a discriminator network that is trained to differentiate between the super-resolved images and original photo-realistic images. In addition, we*

**1. Introduction**

The highly challenging task of estimating a high-resolution (HR) image from its low-resolution (LR) counterpart is referred to as super-resolution (SR). SR received substantial attention from within the computer vision research community and has a wide range of applications [63, 71, 43].

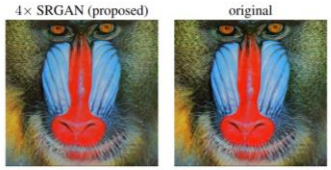


Figure 1: Super-resolved image (left) is almost indistinguishable from original (right). [4× upscaling]

The ill-posed nature of the underdetermined SR problem is particularly pronounced for high upscaling factors, for which texture detail in the reconstructed SR images is typically absent. The optimization target of supervised SR algorithms is commonly the minimization of the mean

SRGAN
(21.15dB/0.6868)

original

*Teco Gan:
https://www.youtube.com/watch?v=pZXFXtfd-Ak&t=45s

**LEARNING TEMPORAL COHERENCE VIA SELF-SUPERVISION FOR GAN-BASED VIDEO GENERATION**

**Mengyu Chu*, You Xie*, Jonas Mayer, Laura Leal-Taixé, Nils Thuerey**
Department of Computer Science
Technical University of Munich
Munich, Germany
{mengyu.chu, you.xie, jonas.a.mayer, leal.taixe, nils.thuerey}@tum.de

ABSTRACT

We focus on temporal self-supervision for GAN-based video generation tasks. While adversarial training successfully yields generative models for a variety of

# GAN Applications: Image Colorization

## Image Colorization using Generative Adversarial Networks

Kamyar Nazeri, Eric Ng, and Mehran Ebrahimi

Faculty of Science, University of Ontario Institute of Technology
2000 Simcoe Street North, Oshawa, Ontario, Canada L1H 7K4
{kamyar.nazeri,eric.ng,mehran.ebrahimi}@uoit.ca
http://www.ImagingLab.ca/

**Abstract.** Over the last decade, the process of automatic image colorization has been of significant interest for several application areas including restoration of aged or degraded images. This problem is highly ill-posed due to the large degrees of freedom during the assignment of color information. Many of the recent developments in automatic colorization involve images that contain a common theme or require highly processed data such as semantic maps as input. In our approach, we attempt to fully generalize the colorization procedure using a conditional Deep Convolutional Generative Adversarial Network (DCGAN). The network is trained over datasets that are publicly available such as CIFAR-10 and Places365. The results between the generative model and traditional deep neural networks are compared.

### 1 Introduction

The automatic colorization of grayscale images has been an active area of research in machine learning for an extensive period of time. This is due to the large variety of applications such color restoration and image colorization for animations. In this manuscript, we will explore the method of colorization using generative adversarial networks (GANs) proposed by Goodfellow et al. [1]. The network is trained on the datasets CIFAR-10 and Places365 [2] and its results will be compared with those obtained using existing convolutional neural networks (CNN).

Models for the colorization of grayscales began back in the early 2000s. In 2002, Welsh et al. [3] proposed an algorithm that colorized images through texture synthesis. Colorization was done by matching luminance and texture information between an existing color image and the grayscale image to be colorized. However, this proposed algorithm was defined as a forward problem, thus all solutions were deterministic. Levin et al. [4] proposed an alternative formulation to the colorization problem in 2004. This formulation followed an inverse approach, where the cost function was designed by penalizing the difference between each pixel and a weighted average of its neighboring pixels. Both of these proposed methods still required significant user intervention which made the solutions less than ideal.

# GAN Applications: 3D GANs

## Learning a Probabilistic Latent Space of Object Shapes via 3D Generative-Adversarial Modeling

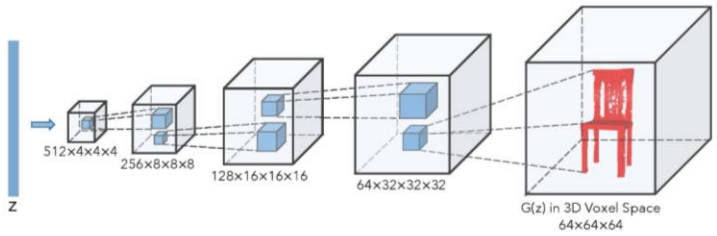


Figure 1: The generator of 3D Generative Adversarial Networks (3D-GAN)

Figure 2: Shapes synthesized by 3D-GAN

**Abstract**

We study the problem of 3D object generation. We propose a novel framework, namely 3D Generative Adversarial Network (3D-GAN), which generates 3D objects from a probabilistic space by leveraging recent advances in volumetric convolutional networks and generative adversarial nets. The benefits of our model are three-fold: first, the use of an adversarial criterion, instead of traditional heuristic criteria, enables the generator to capture object structure implicitly and to synthesize high-quality 3D objects; second, the generator establishes a mapping from a low-dimensional probabilistic space to the space of 3D objects, so that we can sample objects without a reference image or CAD models, and explore the 3D object manifold; third, the adversarial discriminator provides a powerful 3D shape descriptor which, learned without supervision, has wide applications in 3D object recognition. Experiments demonstrate that our method generates high-quality 3D objects, and our unsupervisedly learned features achieve impressive performance on 3D object recognition, comparable with those of supervised learning methods.

https://www.youtube.com/watch?v=mfx7uAkUtCI

# GAN Applications: GauGAN

**Semantic Image Synthesis with Spatially-Adaptive Normalization**

Taesung Park[1,2*] Ming-Yu Liu[2] Ting-Chun Wang[2] Jun-Yan Zhu[2,3]

[1]UC Berkeley [2]NVIDIA [2,3]MIT CSAIL

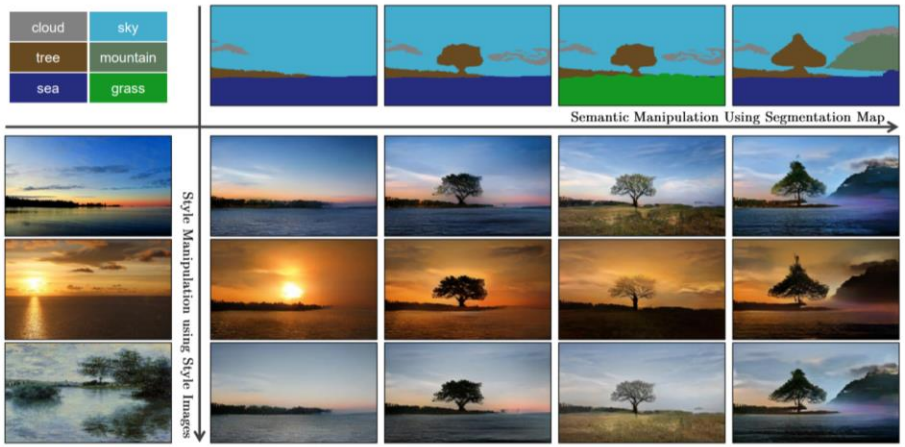


Figure 1: Our model allows user control over both semantic and style as synthesizing an image. The semantic (e.g., the existence of a tree) is controlled via a label map (the top row), while the style is controlled via the reference style image (the leftmost column). Please visit our website for interactive image synthesis demos.

**Abstract**

*We propose spatially-adaptive normalization, a simple but effective layer for synthesizing photorealistic images given an input semantic layout. Previous methods directly feed the semantic layout as input to the deep network, which is then processed through stacks of convolution, normalization, and nonlinearity layers. We show that this is suboptimal as the normalization layers tend to "wash away" semantic information. To address the issue, we propose using the input layout for modulating the activations in normal-*

https://github.com/NVlabs/SPADE.

## 1. Introduction

Conditional image synthesis refers to the task of generating photorealistic images conditioning on certain input data. Seminal work computes the output image by stitching pieces from a single image (e.g., Image Analogies [16]) or using an image collection [7, 14, 23, 30, 35]. Recent methods directly learn the mapping using neural networks [3, 6, 22, 47, 48, 54, 55, 56]. The latter methods are

http://nvidia-research-mingyuliu.com/gaugan/

# GAN Applications: Text/ Caption Generation

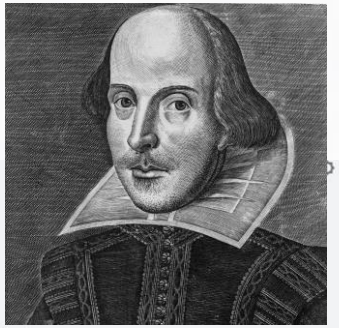

**Generating Diverse and Accurate Visual Captions by Comparative Adversarial Learning**

**Dianqi Li**[1]*, **Qiuyuan Huang**[2], **Xiaodong He**[3]*, **Lei Zhang**[2], **Ming-Ting Sun**[1]
[1]University of Washington, [2]Microsoft Research, [3]JD AI Research
{dianqili, mts}@uw.edu, xiaodong.he@jd.com, {leizhang, qihua}@microsoft.com

| | | | | |
|---|---|---|---|---|
| Pizza |  |  |  |  |
| MLE | a pizza sitting on top of a white plate | a pizza sitting on top of a white plate | a close up of a pizza on a table | a pizza sitting on top of a pan |
| G-GAN | a pizza on a plate on a wooden table | a pizza sitting on a plate next to a glass of wine | the pizza is covered with cheese and tomatoes | a close up of a sliced pizza on a plate |
| CAL | a cheese pizza on a plate sits on a table | a plate of pizza and a glass of beer on the table | a pizza topped with lots of toppings is ready to be cut | a partially eaten pizza is being cooked on a pan |
| Car |  |  |  |  |
| MLE | a green truck parked in a parking lot | a black truck is parked in a parking lot | a group of buses driving down a street | a city bus stopped at a bus stop |
| G-GAN | a green garbage truck in a business district | an antique black car sitting in a parking lot | a city street filled with taxis and buses | people are waiting in line as the bus travel down the road |
| CAL | a large green truck driving past a tall building | an old style truck parked in a parking space near a building | the city buses are driving through the traffic | people gather to a street where a bus get ready to board |

```
QUEENE:
I had thought thou hadst a Roman; for the oracle,
Thus by All bids the man against the word,
Which are so weak of care, by old care done;
Your children were in your holy love,
And the precipitation through the bleeding throne.

BISHOP OF ELY:
Marry, and will, my lord, to weep in such a one were prettiest;
Yet now I was adopted heir
Of the world's lamentable day,
To watch the next way with his father with his face?

ESCALUS:
The cause why then we are all resolved more sons.

VOLUMNIA:
O, no, no, no, no, no, no, no, no, no, no, no, no, no, no, no, no, no, no, no, no, it is no sin it shoul
And love and pale as any will to that word.

QUEEN ELIZABETH:
But how long have I heard the soul for this world,
And show his hands of life be proved to stand.

PETRUCHIO:
I say he look'd on, if I must be content
To stay him from the fatal of our country's bliss.
His lordship pluck'd from this sentence then for prey,
And then let us twain, being the moon,
were she such a case as fills m
```

$$\sum_{k=1}^{\infty} P(E_k) = \sum_{k=1}^{\infty} p = \infty$$

# GAN Applications: Image Generation from Text

**AttnGAN: Fine-Grained Text to Image Generation with Attentional Generative Adversarial Networks**

Tao Xu*[1], Pengchuan Zhang[2], Qiuyuan Huang[2],
Han Zhang[3], Zhe Gan[4], Xiaolei Huang[1], Xiaodong He[5]

[1]Lehigh University [2]Microsoft Research [3]Rutgers University [4]Duke University [5]JD AI Research
{tax313, xih206}@lehigh.edu, {penzhan, qihua, xiaohe}@microsoft.com
han.zhang@cs.rutgers.edu, zhe.gan@duke.edu, xiaodong.he@jd.com

**Abstract**

*In this paper, we propose an Attentional Generative Adversarial Network (AttnGAN) that allows attention-driven, multi-stage refinement for fine-grained text-to-image generation. With a novel attentional generative network, the AttnGAN can synthesize fine-grained details at different subregions of the image by paying attentions to the relevant words in the natural language description. In addition, a deep attentional multimodal similarity model is proposed to compute a fine-grained image-text matching loss for training the generator. The proposed AttnGAN significantly outperforms the previous state of the art, boosting the best reported inception score by 14.14% on the CUB dataset and 170.25% on the more challenging COCO dataset. A detailed analysis is also performed by visualizing the attention layers of the AttnGAN. It for the first time shows that the layered attentional GAN is able to automatically select the condition at the word level for generating different parts of the image.*

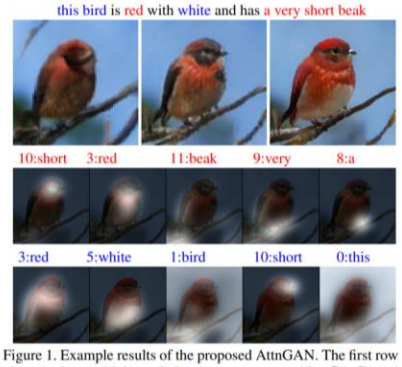


Figure 1. Example results of the proposed AttnGAN. The first row gives the low-to-high resolution images generated by $G_0$, $G_1$ and $G_2$ of the AttnGAN; the second and third row shows the top-5 most attended words by $F_1^{attn}$ and $F_2^{attn}$ of the AttnGAN, respectively. Here, images of $G_0$ and $G_1$ are bilinearly upsampled to have the same size as that of $G_2$ for better visualization.

**1. Introduction**

Automatically generating images according to natural language descriptions is a fundamental problem in many applications, such as art generation and computer-aided design. It also drives research progress in multimodal learning and inference across vision and language, which is one of the most active research areas in recent years [20, 18, 36, 19, 41, 4, 30, 5, 1, 31, 33, 32]

Most recently proposed text-to-image synthesis methods are based on Generative Adversarial Networks (GANs) [6]. A commonly used approach is to encode the whole text description into a global sentence vector as the condition for ... only on the global sentence vector lacks important fine-grained information at the word level, and prevents the generation of high quality images. This problem becomes even more severe when generating complex scenes such as those in the COCO dataset [14].

To address this issue, we propose an Attentional Generative Adversarial Network (AttnGAN) that allows attention-driven, multi-stage refinement for fine-grained text-to-image generation. The overall architecture of the AttnGAN

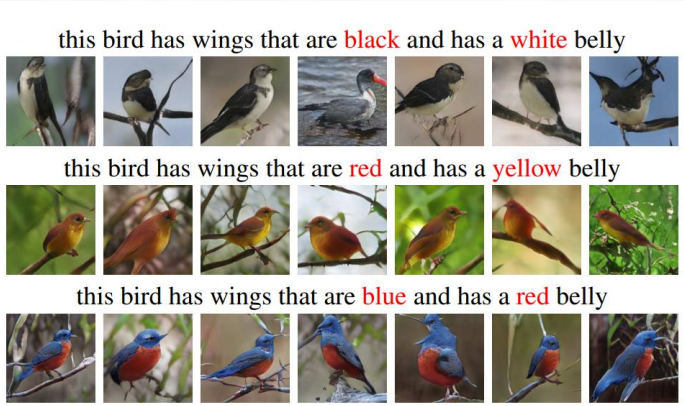


Figure 5. Example results of our AttnGAN model trained on CUB while changing some most attended words in the text descriptions.


Figure 6. 256×256 images generated from descriptions of novel scenarios using the AttnGAN model trained on COCO. (Intermediate results are given in the supplementary material.)

https://openaccess.thecvf.com/content_cvpr_2018/papers/Xu_AttnGAN_Fine-Grained_Text_CVPR_2018_paper.pdf

# GAN Applications: Music Generation

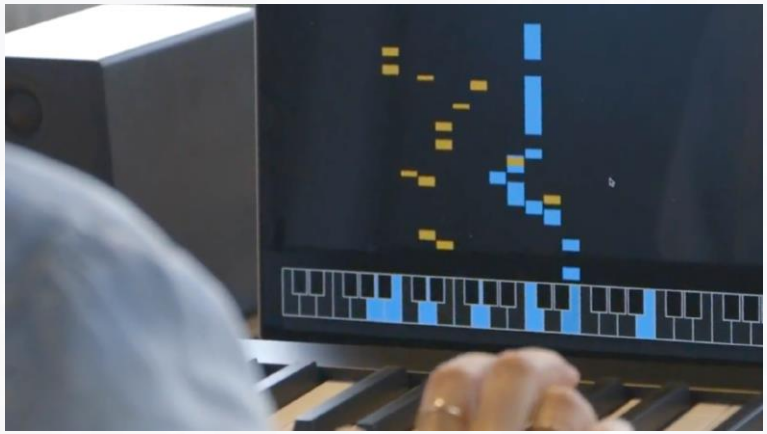

https://experiments.withgoogle.com/ai/ai-duet/view/

GANSynth:
Adversarial Neural Audio Synthesis

**Jesse Engel, Kumar Krishna Agrawal, Shuo Chen, Ishaan Gulrajani, Chris Donahue, & Adam Roberts**
Google AI
Mountain View, CA 94043, USA

Abstract

Efficient audio synthesis is an inherently difficult machine learning task, as human perception is sensitive to both global structure and fine-scale waveform coherence. Autoregressive models, such as WaveNet, model local structure but have slow iterative sampling and lack global latent structure. In contrast, Generative Adversarial Networks (GANs) have global latent conditioning and efficient parallel sampling, but struggle to generate locally-coherent audio waveforms. Herein, we demonstrate that GANs can in fact generate high-fidelity and locally-coherent audio by modeling log magnitudes and instantaneous frequencies with sufficient frequency resolution in the spectral domain. Through extensive empirical investigations on the NSynth dataset, we demonstrate that GANs are able to outperform strong WaveNet baselines on automated and human evaluation metrics, and efficiently generate audio several orders of magnitude faster than their autoregressive counterparts.[1]

## 1 Introduction

*Neural audio synthesis*, training generative models to efficiently produce audio with both high-fidelity and global structure, is a challenging open problem as it requires modeling temporal scales over at least five orders of magnitude (~0.1ms to ~100s). Large advances in the state-of-the art have been pioneered almost exclusively by autoregressive models, such as WaveNet, which solve

https://storage.googleapis.com/magentadata/papers/gansynth/index.html

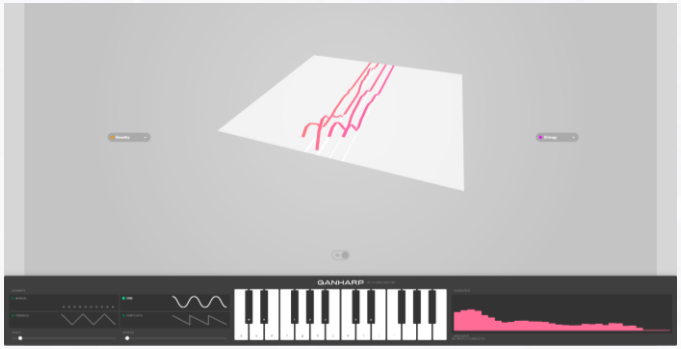


https://ganharp.ctpt.co/

# GAN Applications: OpenAI Jukebox

## Jukebox: A Generative Model for Music

Prafulla Dhariwal [*1] Heewoo Jun [*1] Christine Payne [*1] Jong Wook Kim [1] Alec Radford [1] Ilya Sutskever [1]

**Abstract**

We introduce Jukebox, a model that generates music with singing in the raw audio domain. We tackle the long context of raw audio using a multi-scale VQ-VAE to compress it to discrete codes, and modeling those using autoregressive Transformers. We show that the combined model at scale can generate high-fidelity and diverse songs with coherence up to multiple minutes. We can condition on artist and genre to steer the musical and vocal style, and on unaligned lyrics to make the singing more controllable. We are releasing thousands of non cherry-picked samples, along with model weights and code.

### 1. Introduction

Music is an integral part of human culture, existing from the earliest periods of human civilization and evolving into a wide diversity of forms. It evokes a unique human spirit in its creation, and the question of whether computers can ever capture this creative process has fascinated computer scientists for decades. We have had algorithms generating piano sheet music (Hiller Jr & Isaacson, 1957; Moorer, 1972; Hadjeres et al., 2017; Huang et al., 2017), digital vocoders generating a singer's voice (Bonada & Serra, 2007; Saino et al., 2006; Blaauw & Bonada, 2017) and also synthesizers producing timbres for various musical instruments (Engel et al., 2017; 2019). Each captures a specific aspect of music generation: melody, composition, timbre, and the human voice singing. However, a single system to do it all remains elusive.

The field of generative models has made tremendous progress in the last few years. One of the aims of generative modeling is to capture the salient aspects of the data and to generate new instances indistinguishable from the true data The hypothesis is that by learning to produce the oped advances in text generation (Radford et al.), speech generation (Xie et al., 2017) and image generation (Brock et al., 2019; Razavi et al., 2019). The rate of progress in this field has been rapid, where only a few years ago we had algorithms producing blurry faces (Kingma & Welling, 2014; Goodfellow et al., 2014) but now we now can generate high-resolution faces indistinguishable from real ones (Zhang et al., 2019b).

Generative models have been applied to the music generation task too. Earlier models generated music symbolically in the form of a pianoroll, which specifies the timing, pitch, velocity, and instrument of each note to be played. (Yang et al., 2017; Dong et al., 2018; Huang et al., 2019a; Payne, 2019; Roberts et al., 2018; Wu et al., 2019). The symbolic approach makes the modeling problem easier by working on the problem in the lower-dimensional space. However, it constrains the music that can be generated to being a specific sequence of notes and a fixed set of instruments to render with. In parallel, researchers have been pursuing the non-symbolic approach, where they try to produce music directly as a piece of audio. This makes the problem more challenging, as the space of raw audio is extremely high dimensional with a high amount of information content to model. There has been some success, with models producing piano pieces either in the raw audio domain (Oord et al., 2016; Mehri et al., 2017; Yamamoto et al., 2020) or in the spectrogram domain (Vasquez & Lewis, 2019). The key bottleneck is that modeling the raw audio directly introduces extremely long-range dependencies, making it computationally challenging to learn the high-level semantics of music. A way to reduce the difficulty is to learn a lower-dimensional encoding of the audio with the goal of losing the less important information but retaining most of the musical information. This approach has demonstrated some success in generating short instrumental pieces restricted to a set of a few instruments (Oord et al., 2017; Dieleman et al., 2018).

In this work, we show that we can use state-of-the-art deep

https://arxiv.org/pdf/2005.00341.pdf

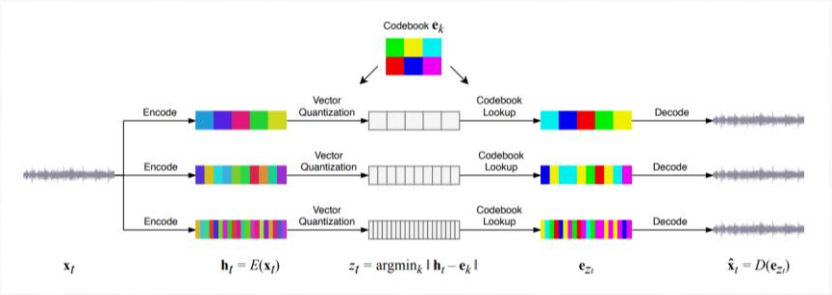


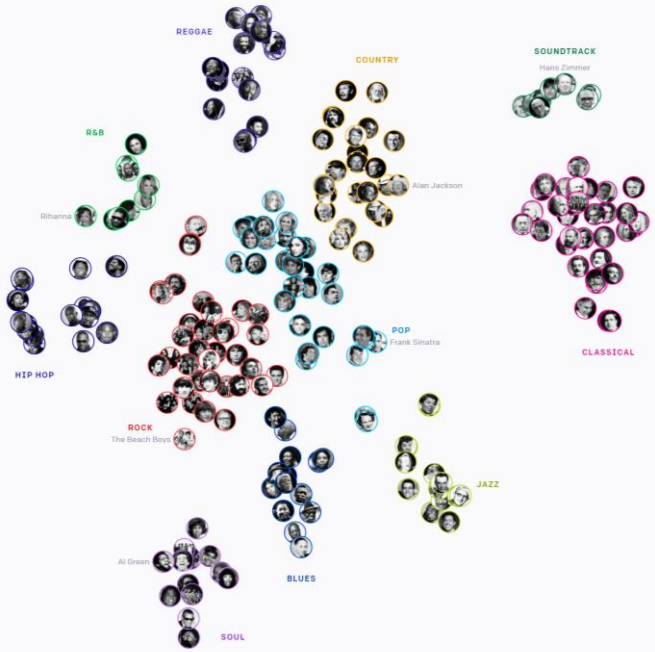


https://jukebox.openai.com/

# GAN FAILS

A perfectly normal human boy|

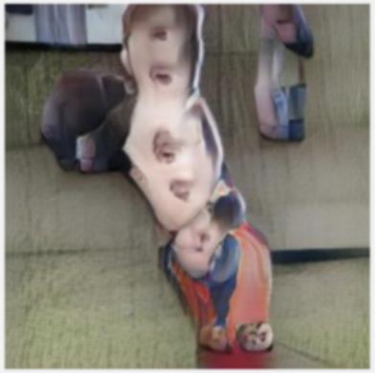



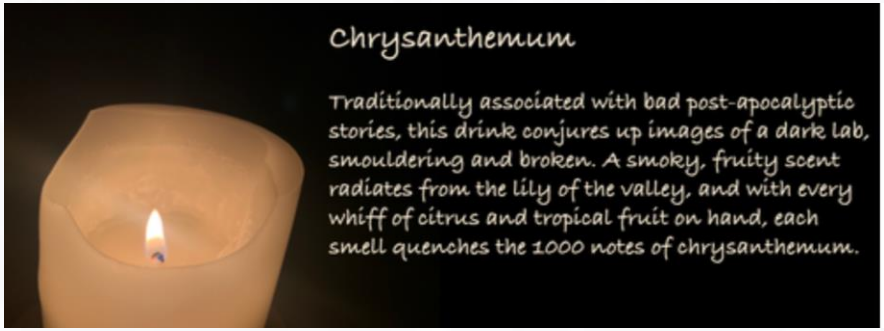


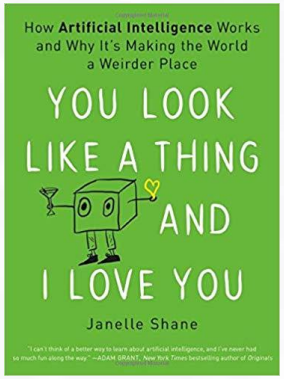

# VAE Background: Autoencoders

- Kingma and Welling published "Auto-Encoding Variational Bayes"* in 2013.

- Recall that an Autoencoder (AE) is a (symmetric) feed-forward NN containing a **bottleneck layer** and trained using **reconstruction loss**.

- AE can naturally be divided into two comparable components: An **encoder network** and a **decoder network**. The encoder induces a form of dimensionality reduction (e.g., PCA), while the decoder can be used to generate synthetic data.

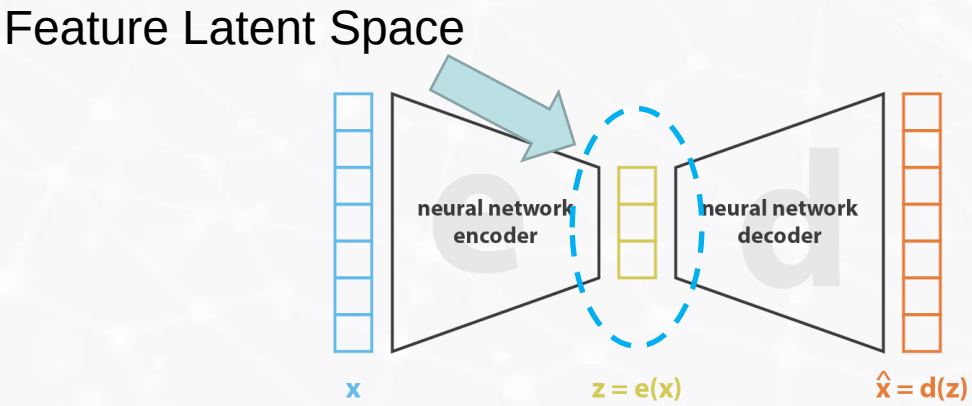


$$\text{loss} = \|x - \hat{x}\|^2 = \|x - d(z)\|^2 = \|x - d(e(x))\|^2$$

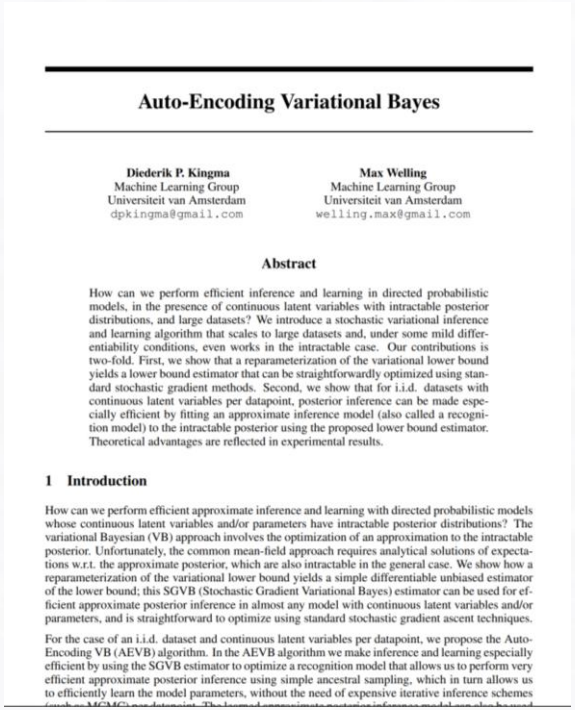

Auto-Encoding Variational Bayes

Diederik P. Kingma
Machine Learning Group
Universiteit van Amsterdam
dpkingma@gmail.com

Max Welling
Machine Learning Group
Universiteit van Amsterdam
welling.max@gmail.com

Abstract

How can we perform efficient inference and learning in directed probabilistic models, in the presence of continuous latent variables with intractable posterior distributions, and large datasets? We introduce a stochastic variational inference and learning algorithm that scales to large datasets and, under some mild differentiability conditions, even works in the intractable case. Our contributions is two-fold. First, we show that a reparameterization of the variational lower bound yields a lower bound estimator that can be straightforwardly optimized using standard stochastic gradient methods. Second, we show that for i.i.d. datasets with continuous latent variables per datapoint, posterior inference can be made especially efficient by fitting an approximate inference model (also called a recognition model) to the intractable posterior using the proposed lower bound estimator. Theoretical advantages are reflected in experimental results.

1 Introduction

How can we perform efficient approximate inference and learning with directed probabilistic models whose continuous latent variables and/or parameters have intractable posterior distributions? The variational Bayesian (VB) approach involves the optimization of an approximation to the intractable posterior. Unfortunately, the common mean-field approach requires analytical solutions of expectations w.r.t. the approximate posterior, which are also intractable in the general case. We show how a reparameterization of the variational lower bound yields a simple differentiable unbiased estimator of the lower bound; this SGVB (Stochastic Gradient Variational Bayes) estimator can be used for efficient approximate posterior inference in almost any model with continuous latent variables and/or parameters, and is straightforward to optimize using standard stochastic gradient ascent techniques.

For the case of an i.i.d. dataset and continuous latent variables per datapoint, we propose the Auto-Encoding VB (AEVB) algorithm. In the AEVB algorithm we make inference and learning especially efficient by using the SGVB estimator to optimize a recognition model that allows us to perform very efficient approximate posterior inference using simple ancestral sampling, which in turn allows us to efficiently learn the model parameters, without the need of expensive iterative inference schemes

*https://arxiv.org/pdf/1312.6114.pdf

# VAE Background: Autoencoders

• Importantly, variational autoencoders (VAEs) add a stochastic mechanism (a **random vector**) that enables the network to generate synthetic outputs; additionally, VAEs **regularize the latent space**.

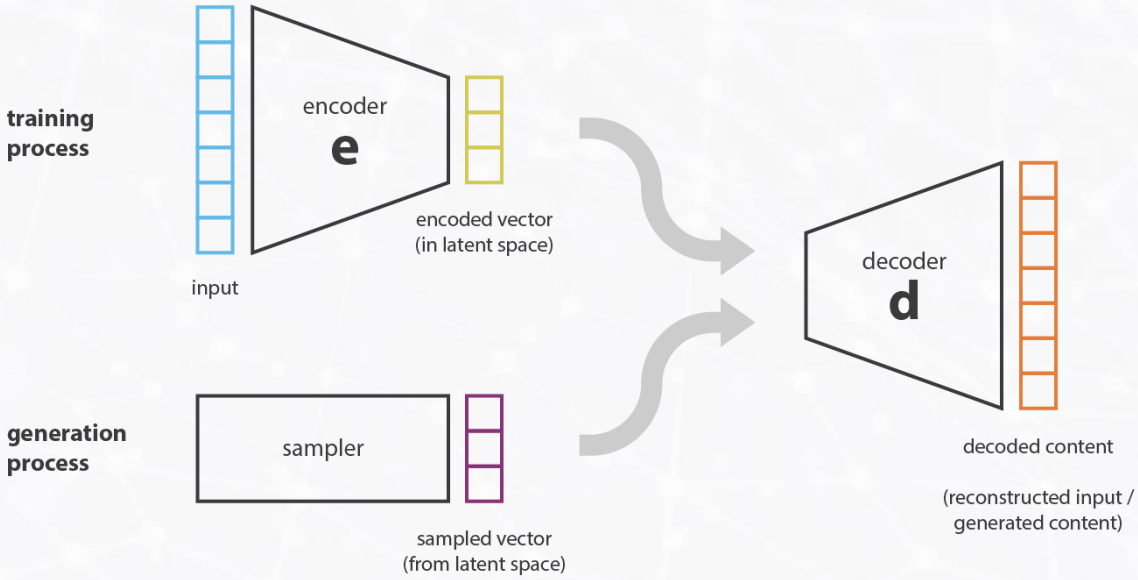

# VAE Background: Variational Inference (brief)

• The goal of **variational inference** is to approximate a conditional density of **latent variables** (denoted z), given **observed variables** (denoted x), using optimization. This conditional density can be used to produce point or interval estimates for latent variables, form predictive densities of new data, etc.

• As usual, we can write the conditional density as:

$$p(z \mid x) = \frac{p(z, x)}{p(x)}$$

# VAE Background: Variational Inference

$$p(z \mid x) = \frac{p(z, x)}{p(x)}$$

• Here the denominator contains the marginal density of the observations, also known as the **evidence**. We can calculate the evidence by marginalizing out the latent variables:

$$p(x) = \int p(z, x) dz$$

• In many cases, this integral is intractable and so we must resort to approximation techniques. On the one hand, we can use Monte Carlo techniques to generate a numerical approximation to the exact posterior using samples.

• By contrast, variational inference provides an analytical solution to the posterior distribution.

# VAE Background: Variational Inference

$$p(z \mid x) = \frac{p(z, x)}{p(x)}$$

• In variational inference, we specify a family Q of density functions (e.g., Gaussians) over latent variables. Each $q(z) \in Q$ is a candidate approximation to the exact conditional.

• Our goal is to find the best candidate, i.e., the one closest in KL divergence to the exact conditional. Accordingly, we solve the following optimization problem:

$$q^*(z) = \arg\min_{q(z) \in Q} KL(q(z) \,\|\, p(z \mid x))$$

• Once found, q* is the best approximation for the conditional – within the family Q. The complexity of the family determines the complexity of this optimization problem.

# VAE Background: Variational Inference

$$q^*(z) = \arg\min_{q(z) \in Q} KL(q(z) \,||\, p(z \mid x))$$

• This objective is, however, in general not computable because it requires the aforementioned evidence:

# VAE Background: Variational Inference

$$q^*(z) = \arg\min_{q(z) \in Q} KL(q(z) \,||\, p(z \mid x))$$

• This objective is, however, in general not computable because it requires the aforementioned evidence term:

$$q^*(z) = \arg\min_{q(z) \in Q} KL(q(z) \,||\, p(z \mid x))$$

$$= E_q[\log q(z)] - E_q[\log p(z \mid x)]$$

$$= E_q[\log q(z)] - E_q[\log p(z, x)] + \log p(x)$$

$$p(x) = \int p(z, x) dz$$

# VAE Background: Variational Inference

$$q^*(z) = \arg\min_{q(z) \in Q} KL(q(z) \,||\, p(z \mid x))$$

• Because we cannot compute the KL-divergence directly, we instead optimize an alternative objective that is equivalent to the KL-divergence up to a constant; this alternative function is called the **evidence lower-bound** (ELBO):

# VAE Background: Variational Inference

$$q^*(z) = \arg\min_{q(z) \in Q} KL(q(z) \,||\, p(z \mid x))$$

• Because we cannot compute the KL-divergence directly, we instead optimize an alternative objective that is equivalent to the KL-divergence up to a constant; this alternative function is called the **evidence lower-bound** (ELBO):

$$\text{ELBO(q)} = E_q[\log p(z, x)] - E_q[\log q(z)]$$

$$\begin{aligned} q^*(z) &= \arg\min_{q(z) \in Q} KL(q(z) \,||\, p(z \mid x)) \\ &= E_q[\log q(z)] - E_q[\log p(z, x)] + \log p(x) \end{aligned}$$

• The ELBO is the negative KL divergence of q*, plus log(p(x)) (which is a constant with respect to q(z)).

• **Maximizing the ELBO is equivalent to minimizing the KL-divergence**.

# VAE Background: Variational Inference

$$\text{ELBO(q)}=E_q[\log p(z,x)]-E_q[\log q(z)]$$

- Let's further analyze ELBO:

$$\begin{aligned}\text{ELBO(q)} &= E_q[\log p(z)]+E_q[\log p(x\mid z)]-E_q[\log q(z)]\\ &= E_q[\log p(x\mid z)]-KL(q(z)\,||\,p(z))\end{aligned}$$

- Notice that ELBO is maximal when: (1) the latent variables explain the data (the likelihood expressed by the first term) and (2) when the variational density is close to the prior.

# VAE Background: Variational Inference

$$\text{ELBO(q)}=E_q[\log p(z,x)]-E_q[\log q(z)]$$

• Let's further analyze ELBO:

$$\text{ELBO(q)} = E_q[\log p(z)]+E_q[\log p(x\mid z)]-E_q[\log q(z)]$$

$$= E_q[\log p(x\mid z)]-KL(q(z)\,||\,p(z))$$

• Notice that ELBO is maximal when: (1) the latent variables explain the data (the likelihood expressed by the first term) and (2) when the variational density is close to the prior.

Another property of ELBO is that it lower-bounds the (log) evidence, $\log p(x) \geq ELBO(q)$ for any $q$(z).

To see this, note: $$\log p(x) = KL(q(z)\,||\,p(z\mid x)+ELBO(q)$$

(recall that $KL \geq 0$ – why?)

# VAE

• In summary, **the ELBO defines the objective function underlying variational inference**.

• However, in order to complete the specification of this objective function, we still need to define the ELBO with respect to the previously mentioned family of densities, Q.

# VAE

• In summary, the ELBO defines the objective function underlying variational inference. However, in order to complete the specification of this objective function, we still need to define the ELBO with respect to the previously mentioned family of densities, Q.

• There are, naturally, many different families from which one can choose. In practice, for improved tractability, a common choice is the so-called **mean-field variational family**; for this set of functions, the latent variables are assumed to be mutually independent, so that each is governed by a distinct factor in the variational density.

$$q(z) = \prod_{j=1}^{m} q_j(z_j)$$

# VAE

• Using the ELBO and mean-field family, we have now fully specified the approximate conditional inference problem as an optimization problem.

• In general, maximizing the ELBO is far from trivial. Again, there are many optimization techniques available for this task. One common approach is to use **coordinate ascent variational inference** (CAVI, due to Bishop*). CAVI iteratively optimizes each factor of the mean-field variational density, while holding the others fixed – in this way we arrive at a local optimum for the ELBO.

*See: *Christopher M. Bishop. 2006. Pattern Recognition and Machine Learning (Information Science and Statistics). Springer-Verlag, Berlin, Heidelberg.*

# VAE

• Using the ELBO and mean-field family, we have now fully specified the approximate conditional inference problem as an optimization problem.

• In general, maximizing the ELBO is far from trivial. Again, there are many optimization techniques available for this task. One common approach is to use **coordinate ascent variational inference** (CAVI, due to Bishop*). CAVI iterativly optimizes each factor of the mean-field variational density, while holding the others fixed – in this way we arrive at a local optimum for the ELBO.

**Algorithm 1:** Coordinate ascent variational inference (CAVI)

**Input:** A model $p(\mathbf{x}, \mathbf{z})$, a data set $\mathbf{x}$

**Output:** A variational density $q(\mathbf{z}) = \prod_{j=1}^{m} q_j(z_j)$

**Initialize:** Variational factors $q_j(z_j)$

**while** *the* ELBO *has not converged* **do**

  **for** $j \in \{1, \ldots, m\}$ **do**

    Set $q_j(z_j) \propto \exp\{\mathbb{E}_{-j}[\log p(z_j \mid \mathbf{z}_{-j}, \mathbf{x})]\}$

  **end**

  Compute $\text{ELBO}(q) = \mathbb{E}[\log p(\mathbf{z}, \mathbf{x})] - \mathbb{E}[\log q(\mathbf{z})]$

**end**

**return** $q(\mathbf{z})$

• Where $p(z_j|z_{-j}, x)$ denotes the total is the "total conditional" (i.e., $p(z_j)$ given $x$ and all latent variables except $z_j$, as seen with **Gibbs sampling**.

*See: *Christopher M. Bishop. 2006. Pattern Recognition and Machine Learning (Information Science and Statistics). Springer-Verlag, Berlin, Heidelberg.*

# VAE

• We previously showed that minimizing our VAE objective is equivalent to **maximizing the ELBO**:

$$\text{ELBO(q)} = E_q[\log p(x \mid z)] - KL(q(z \mid x) \,\|\, p(z))$$

# VAE

• We previously showed that minimizing our VAE objective is equivalent to **maximizing the ELBO**:

$$\text{ELBO(q)} = E_q[\log p(x \mid z)] - KL(q(z \mid x) \,\|\, p(z))$$

Notice that the RHS involves (3) quantities:

(1) q(z) (also written q(z|x)) a projection of the data x into the latent space

(2) z, the latent variable

(3) p(x|z) the distribution generating the data, given the latent variable.

• This structure is equivalent to an autoencoder, where q(z|x) is the encoder network; z is the encoded representation, and p(x|z) is the decoder network.

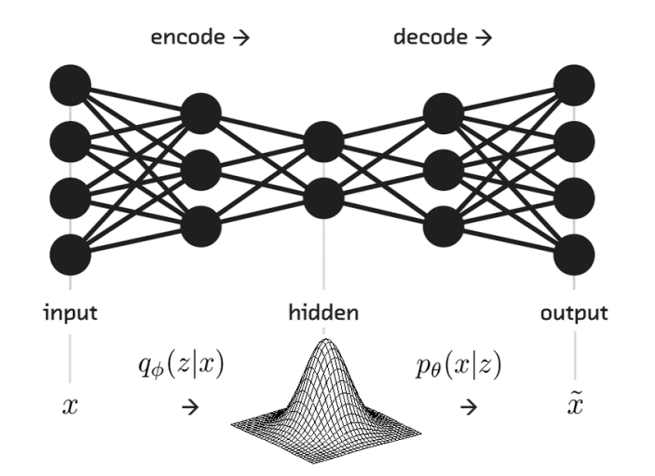

# VAE

$$\text{ELBO(q)} = E_q[\log p(x \mid z)] - KL(q(z \mid x) \,||\, p(z))$$

- For a VAE, we assume that the encoder projects the input to a standard normal (i.e., $\text{q}(z|x) = N(\mu(x), \Sigma(x))$; furthermore, for simplicity, we assume the latent distribution is a standard normal, i.e., $\text{p}(z) = N(0, I)$.

# VAE

$$\text{ELBO(q)} = E_q[\log p(x \mid z)] - KL(q(z \mid x) \,||\, p(z))$$

• For a VAE, we assume that the encoder projects the input to a standard normal (i.e. $\mathrm{q}(z|x) = N(\mu(x), \Sigma(x))$; furthermore, we assume the latent distribution is a standard normal, i.e., $\mathrm{p}(z) = N(0, I)$.

Under these conditions, this KL divergence term admits of a closed-form:

$$\sum_{i=1}^{n} \sigma_i^2 + \mu_i^2 - \log(\sigma_i) - 1$$

• In summary, $\mathrm{q}(z|x)$ is represented by a neural network, where the NN maps input data (x) to a mean vector $\mu(x)$ and (diagonal) covariance matrix $\Sigma(x)$ (the parameters of the latent space).

(*) By minimizing the indicated KL divergence, we encourage the latent space to conform with a standard Normal.

# VAE

$$\text{ELBO}(q) = E_q[\log p(x \mid z)] - KL(q(z \mid x) \,||\, p(z))$$

• Notice that the first term on the RHS is equivalent to MLE; so, **to maximize this term we want to minimize the reconstruction error** of the decoder with respect to a given an input x, the associated encoding z, and the reconstruction of this encoding.

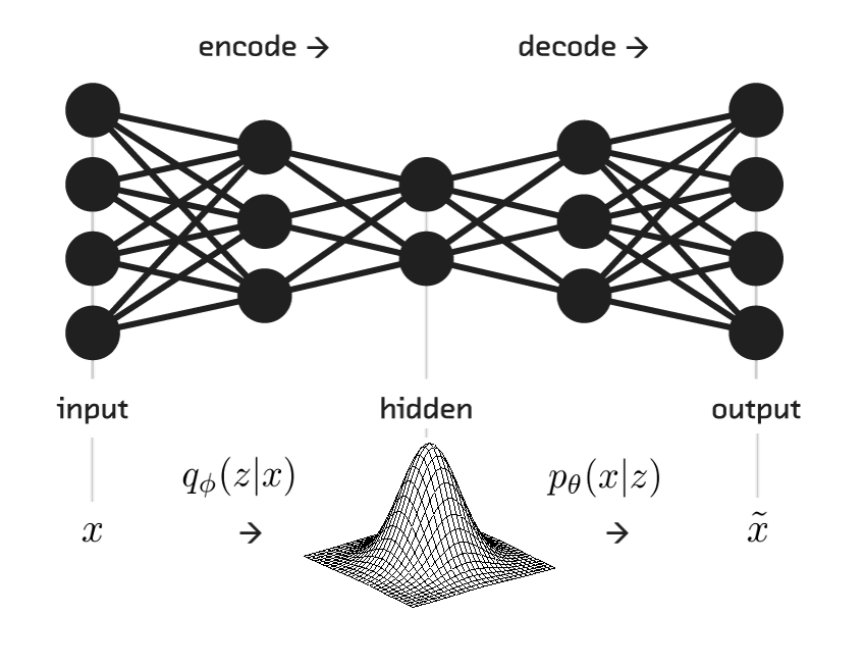

# VAE

• We are almost done – however, recall that we want the latent parameter (z) corresponding with the input (x) to be sampled $z \sim N(\mu(x), \Sigma(x))$.

• However, in order to enable training of the q(z|x) network using backpropagation, the sampling process must exist outside of the network itself. To achieve this, we use the so-call "**reparameterization trick**" (inverse sampling of a Gaussian).

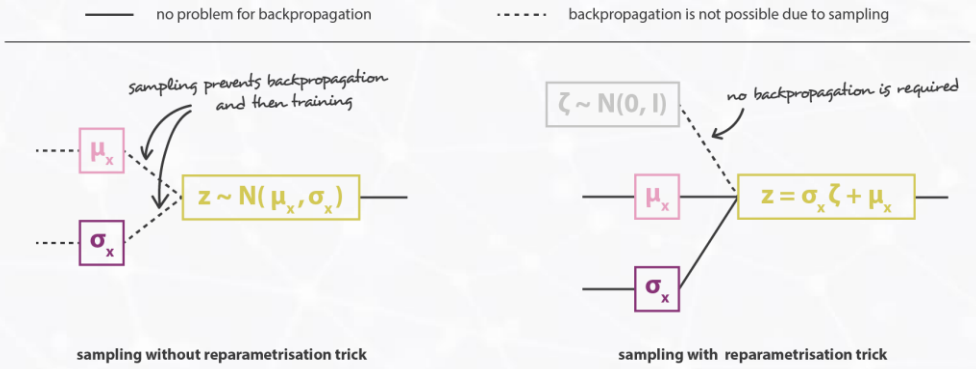


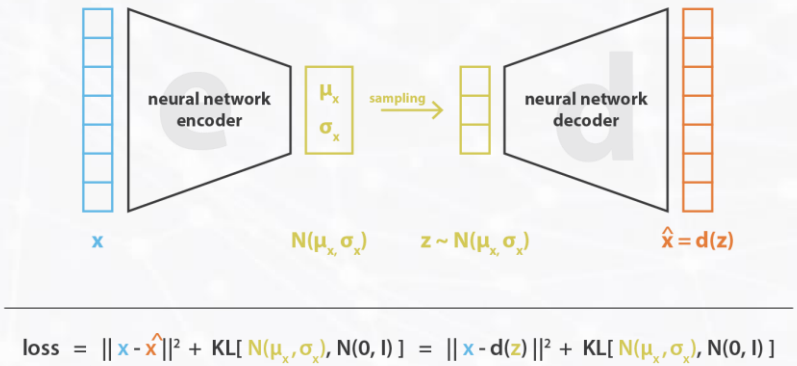


(3) Equivalent to minimizing reconstruction error and KL divergence

$$q^*(z) = \arg\min_{q(z) \in Q} KL(q(z) \,||\, p(z \,|\, x))$$

(1) Want to minimize this

$$\text{ELBO(q)} = E_q[\log p(x \,|\, z)] - KL(q(z \,|\, x) \,||\, p(z))$$

(2) Equivalent to maximizing ELBO

# VAE

• Imposing a structure on the latent space (e.g., Gaussian) is a powerful idea for generative models. This approach has the effect of **regularizing the latent space** (and hence avoiding overfitting to the data).


• Optimizing with both reconstruction loss and KL divergence loss additionally enforces "similarity embedding" – which is to say, similar inputs to the VAE are mapped close to one another in the latent space.

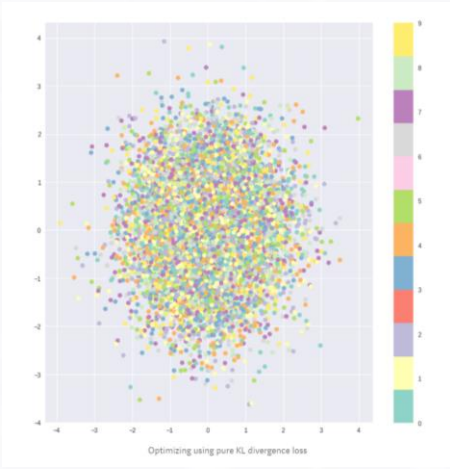


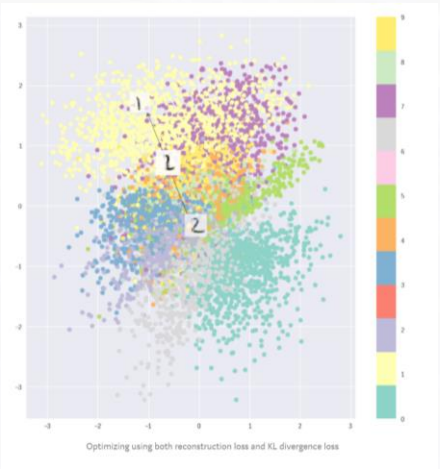

# VAE

- Reconstructing faces with a VAE:

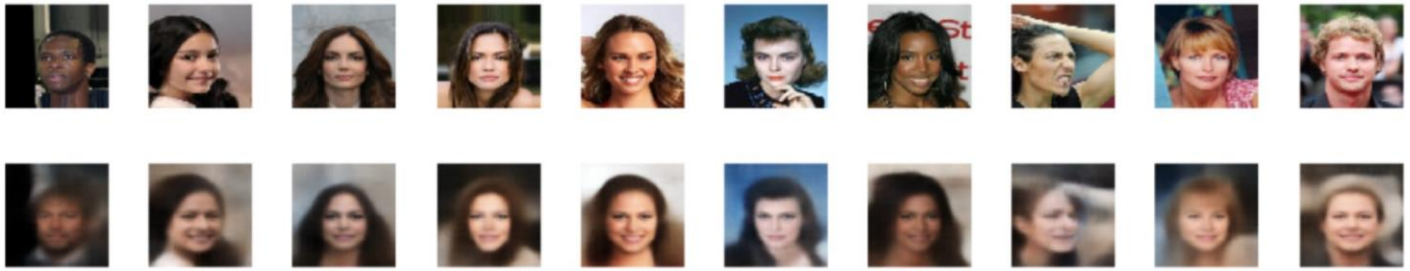

*Figure 3-18. Reconstructed faces, after passing through the encoder and decoder*

- Generating synthetic faces with a VAE:

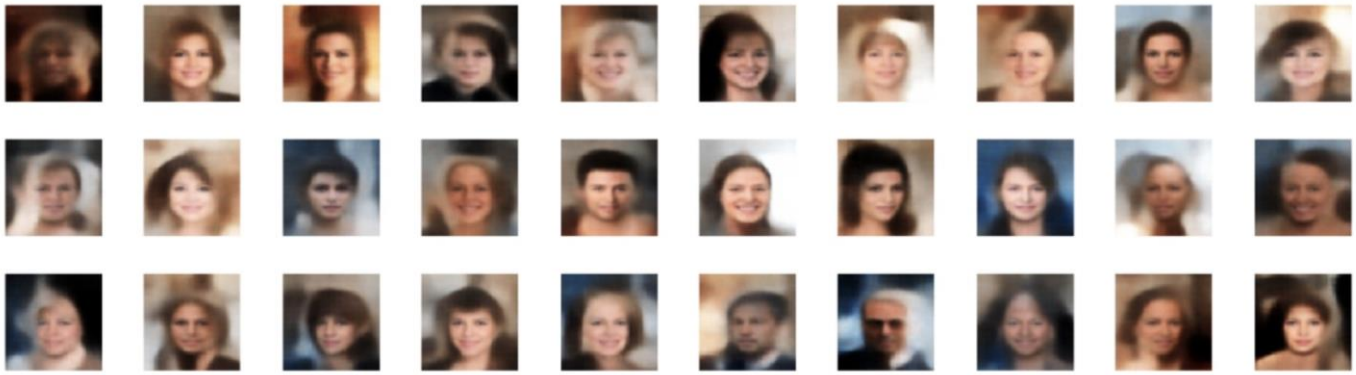

*Figure 3-20. New generated faces*

# VAE: Latent Space Arithmetic

• Notice that it is possible to manipulate the latent space associated with a generative model using **latent space arithmetic**.

•For instance, suppose we wish to vary a particular attribute of our generated synthetic data. The CelebA dataset includes annotations with various attributes, e.g., wearing hat, smiling, etc.

# VAE: Latent Space Arithmetic

• In a similar vein to the latent space arithmetic seen with word-embedding models (e.g., Word2Vec), one can use vector arithmetic to meaningfully augment latent vectors.

• For example, if we want to generate faces that are "smiling", we could in principle take the average latent embedding of all the *faces with the attribute smiling* in our training set and subtract from this the average latent embedding of all the faces *without the attribute smiling*. This gives us a vector in the latent space pointing from "non-smiling" to "smiling".

• Now to apply "smiling" to a latent embedding, we apply the following transformation:

$$\mathbf{z}' = \mathbf{z} + \alpha(\mathbf{feature\_vector})$$

# VAE: Latent Space Arithmetic

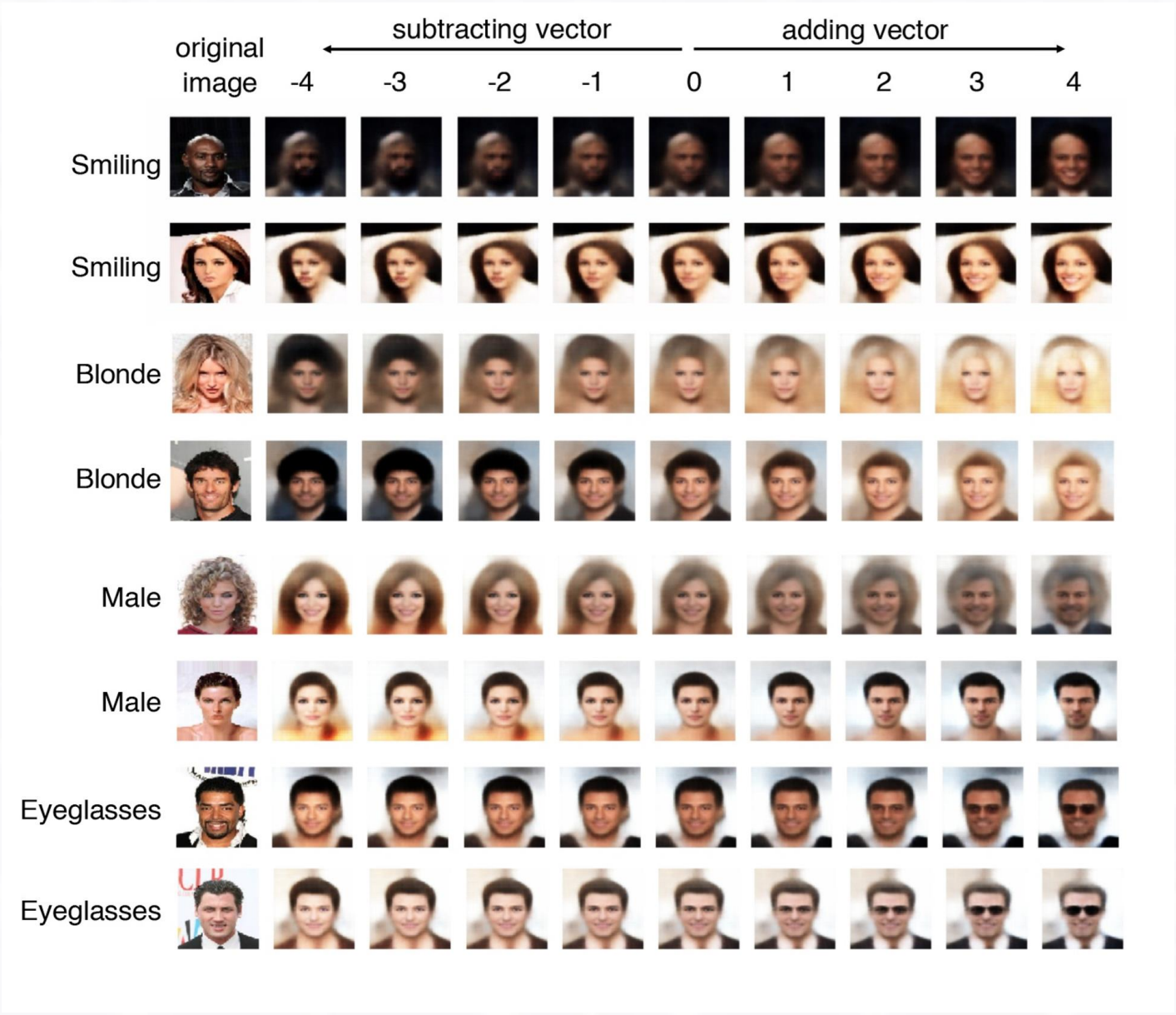

# GAN

• The original GAN paper (Goodfellow *et al,* 2014) is one of the most influential ML papers in recent years.

• Simply put, a GAN is a battle between two adversaries: **the generator** and **the discriminator**.

• The generator attempts to convert random noise into observations that appear as though they were sampled from the original dataset.

• Conversely, the discriminator tries to predict whether an observation comes from the original dataset or is a forgery produced by the generator.

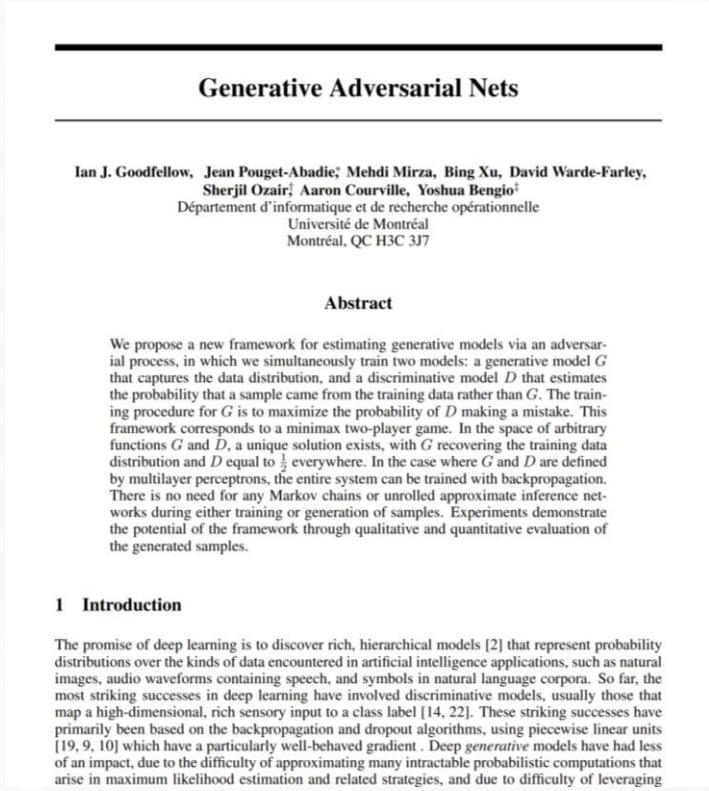

**Generative Adversarial Nets**

**Ian J. Goodfellow, Jean Pouget-Abadie, Mehdi Mirza, Bing Xu, David Warde-Farley, Sherjil Ozair, Aaron Courville, Yoshua Bengio**
Département d'informatique et de recherche opérationnelle
Université de Montréal
Montréal, QC H3C 3J7

**Abstract**

We propose a new framework for estimating generative models via an adversarial process, in which we simultaneously train two models: a generative model $G$ that captures the data distribution, and a discriminative model $D$ that estimates the probability that a sample came from the training data rather than $G$. The training procedure for $G$ is to maximize the probability of $D$ making a mistake. This framework corresponds to a minimax two-player game. In the space of arbitrary functions $G$ and $D$, a unique solution exists, with $G$ recovering the training data distribution and $D$ equal to $\frac{1}{2}$ everywhere. In the case where $G$ and $D$ are defined by multilayer perceptrons, the entire system can be trained with backpropagation. There is no need for any Markov chains or unrolled approximate inference networks during either training or generation of samples. Experiments demonstrate the potential of the framework through qualitative and quantitative evaluation of the generated samples.

**1 Introduction**

The promise of deep learning is to discover rich, hierarchical models [2] that represent probability distributions over the kinds of data encountered in artificial intelligence applications, such as natural images, audio waveforms containing speech, and symbols in natural language corpora. So far, the most striking successes in deep learning have involved discriminative models, usually those that map a high-dimensional, rich sensory input to a class label [14, 22]. These striking successes have primarily been based on the backpropagation and dropout algorithms, using piecewise linear units [19, 9, 10] which have a particularly well-behaved gradient . Deep *generative* models have had less of an impact, due to the difficulty of approximating many intractable probabilistic computations that arise in maximum likelihood estimation and related strategies, and due to difficulty of leveraging

https://arxiv.org/pdf/1406.2661.pdf

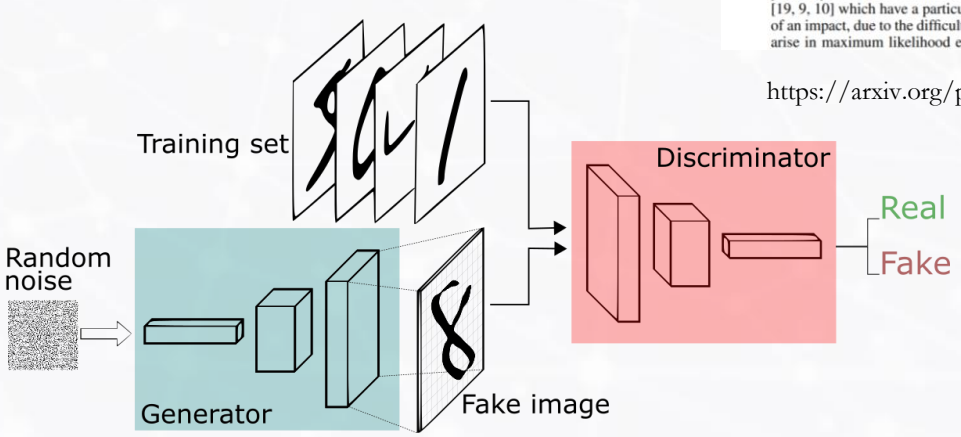

# GAN

• At the beginning of this process, the generator outputs noisy images and the discriminator predicts randomly.

• The key to GANs lies in **how we effect the training of the two networks in tandem**, so that as the generator becomes more adept at fooling the discriminator, the discriminator must adapt in order to maintain its ability to spot "fakes".

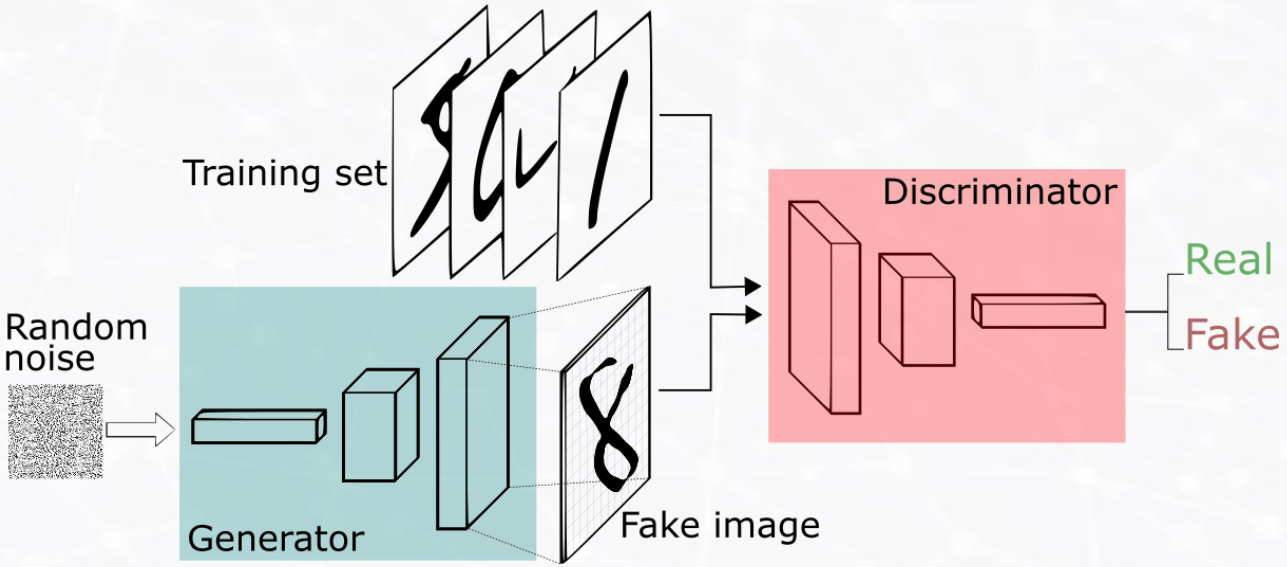

# GAN

• Here's an example specification of a GAN; the architecture of the discriminator is given on the right.

**Discriminator**: define input; stack convolutional layers; flatten the last convolutional layer, etc.; note that a stride of size 2 in the conv layers will reduce the overall size of the tensor; the final "dense" layer (using sigmoid activation) ensures the output is a scalar in the range [0,1], corresponding with the probability that the input image is real.

```
gan = GAN(input_dim = (28,28,1)
          , discriminator_conv_filters = [64,64,128,128]
          , discriminator_conv_kernel_size = [5,5,5,5]
          , discriminator_conv_strides = [2,2,2,1]
          , discriminator_batch_norm_momentum = None
          , discriminator_activation = 'relu'
          , discriminator_dropout_rate = 0.4
          , discriminator_learning_rate = 0.0008
          , generator_initial_dense_layer_size = (7, 7, 64)
          , generator_upsample = [2,2, 1, 1]
          , generator_conv_filters = [128,64, 64,1]
          , generator_conv_kernel_size = [5,5,5,5]
          , generator_conv_strides = [1,1, 1, 1]
          , generator_batch_norm_momentum = 0.9
          , generator_activation = 'relu'
          , generator_dropout_rate = None
          , generator_learning_rate = 0.0004
          , optimiser = 'rmsprop'
          , z_dim = 100
          )
```

| Layer (type) | Output Shape | Param # |
|---|---|---|
| discriminator_input (InputLa | (None, 28, 28, 1) | 0 |
| discriminator_conv_0 (Conv2D | (None, 14, 14, 64) | 1664 |
| activation_1 (Activation) | (None, 14, 14, 64) | 0 |
| dropout_1 (Dropout) | (None, 14, 14, 64) | 0 |
| discriminator_conv_1 (Conv2D | (None, 7, 7, 64) | 102464 |
| activation_2 (Activation) | (None, 7, 7, 64) | 0 |
| dropout_2 (Dropout) | (None, 7, 7, 64) | 0 |
| discriminator_conv_2 (Conv2D | (None, 4, 4, 128) | 204928 |
| activation_3 (Activation) | (None, 4, 4, 128) | 0 |
| dropout_3 (Dropout) | (None, 4, 4, 128) | 0 |
| discriminator_conv_3 (Conv2D | (None, 4, 4, 128) | 409728 |
| activation_4 (Activation) | (None, 4, 4, 128) | 0 |
| dropout_4 (Dropout) | (None, 4, 4, 128) | 0 |
| flatten_1 (Flatten) | (None, 2048) | 0 |
| dense_1 (Dense) | (None, 1) | 2049 |

Total params: 720,833
Trainable params: 720,833
Non-trainable params: 0

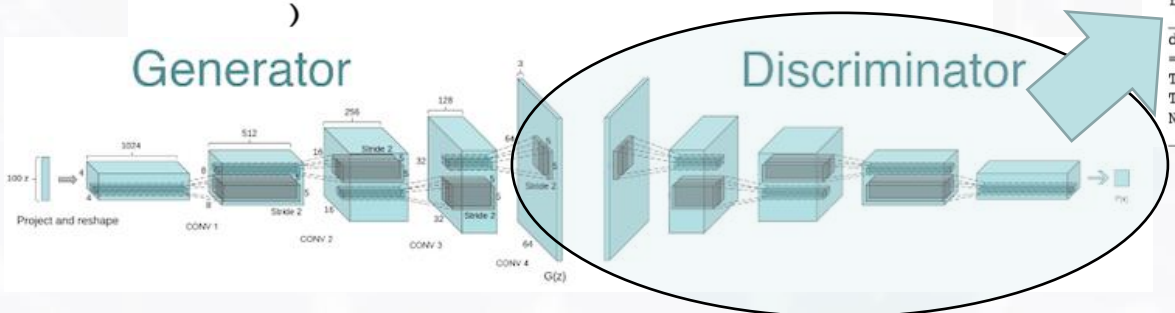

# GAN

• The input to the generator is a vector, usually drawn from a multivariate Normal distribution; the output is an image of the same size as the original dataset.

• The generator serves the same purpose as the decoder for a VAE, in that it converts a vector from the model latent space into an image. The trope of mapping from a low-to-high dimensional space is common in DL; for a CNN, as we have seen, this operation is commonly known as **deconvolution** (also: **transposed convolution**).

| Layer (type) | Output Shape | Param # |
|---|---|---|
| generator_input (InputLayer) | (None, 100) | 0 |
| dense_9 (Dense) | (None, 3136) | 316736 |
| batch_normalization_10 (Batc | (None, 3136) | 12544 |
| activation_36 (Activation) | (None, 3136) | 0 |
| reshape_4 (Reshape) | (None, 7, 7, 64) | 0 |
| up_sampling2d_10 (UpSampling | (None, 14, 14, 64) | 0 |
| generator_conv_0 (Conv2D) | (None, 14, 14, 128) | 204928 |
| batch_normalization_11 (Batc | (None, 14, 14, 128) | 512 |
| activation_37 (Activation) | (None, 14, 14, 128) | 0 |
| up_sampling2d_11 (UpSampling | (None, 28, 28, 128) | 0 |
| generator_conv_1 (Conv2D) | (None, 28, 28, 64) | 204864 |
| batch_normalization_12 (Batc | (None, 28, 28, 64) | 256 |
| activation_38 (Activation) | (None, 28, 28, 64) | 0 |
| generator_conv_2 (Conv2D) | (None, 28, 28, 64) | 102464 |
| batch_normalization_13 (Batc | (None, 28, 28, 64) | 256 |
| activation_39 (Activation) | (None, 28, 28, 64) | 0 |
| generator_conv_3 (Conv2D) | (None, 28, 28, 1) | 1601 |
| activation_40 (Activation) | (None, 28, 28, 1) | 0 |

Total params: 844,161
Trainable params: 837,377
Non-trainable params: 6,784

```
gan = GAN(input_dim = (28,28,1)
          , discriminator_conv_filters = [64,64,128,128]
          , discriminator_conv_kernel_size = [5,5,5,5]
          , discriminator_conv_strides = [2,2,2,1]
          , discriminator_batch_norm_momentum = None
          , discriminator_activation = 'relu'
          , discriminator_dropout_rate = 0.4
          , discriminator_learning_rate = 0.0008
          , generator_initial_dense_layer_size = (7, 7, 64)
          , generator_upsample = [2,2, 1, 1]
          , generator_conv_filters = [128,64, 64,1]
          , generator_conv_kernel_size = [5,5,5,5]
          , generator_conv_strides = [1,1, 1, 1]
          , generator_batch_norm_momentum = 0.9
          , generator_activation = 'relu'
          , generator_dropout_rate = None
          , generator_learning_rate = 0.0004
          , optimiser = 'rmsprop'
          , z_dim = 100
          )
```

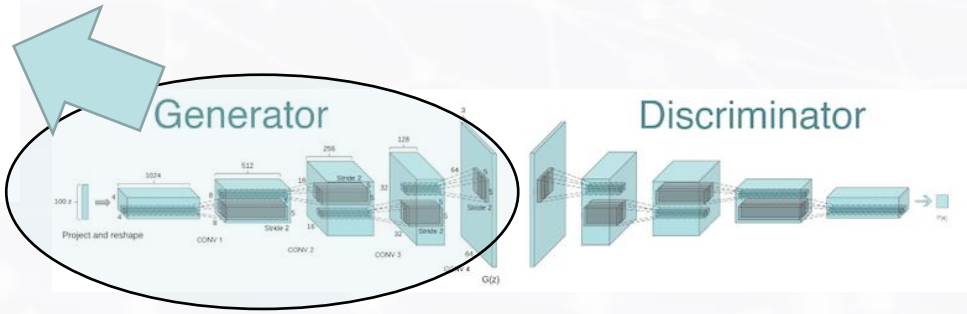

# GAN: Transposed Convolution

• The transposed convolution operation is effected by performing a "backward strided convolution".

• In the images below, the blue maps are inputs; cyan maps are outputs.

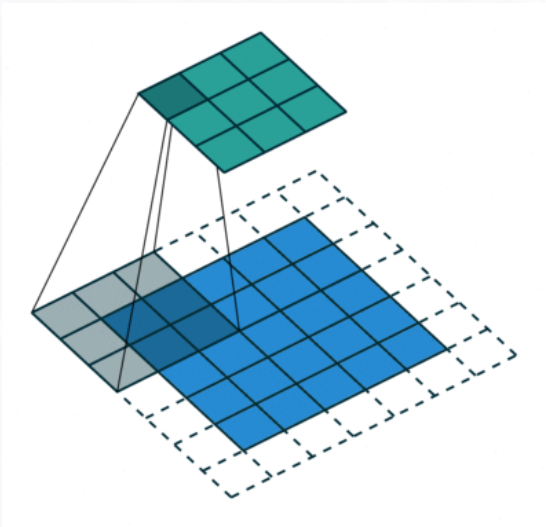

Basic convolution with padding=1, stride =2

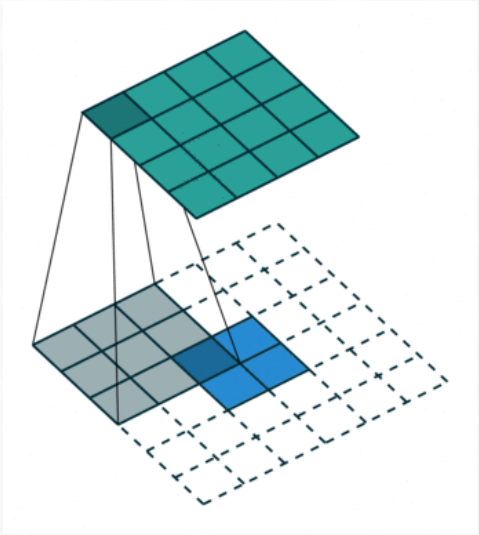

Transposed conv with no padding, no stride

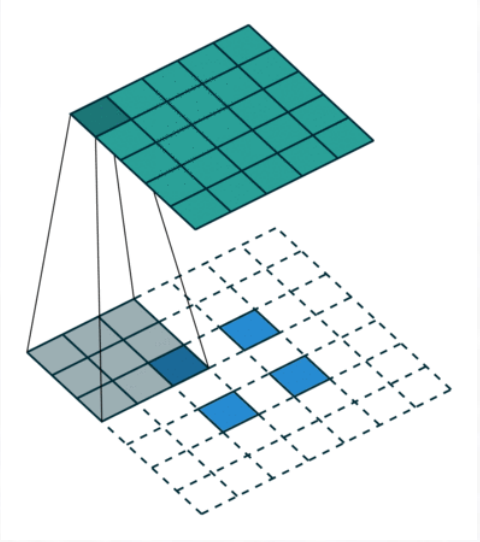

Transposed conv with no padding and stride

• Traditionally, one could achieve up-sampling by applying interpolation schemes (e.g. bilinear interpolation). Modern architectures such as NNs, however, **tend to let the network itself learn the proper transformation automatically**, without human intervention.

# GAN: Transposed Convolution

• Let's dive a little deeper into the contrast between convolution and transposed convolution.
• With convolution, consider *C* as the kernel, *Large* as the input, and *Small* as the output image after convolution. Following convolution, we down-sample the large image into a small output image, i.e., **C x Large = Small**.

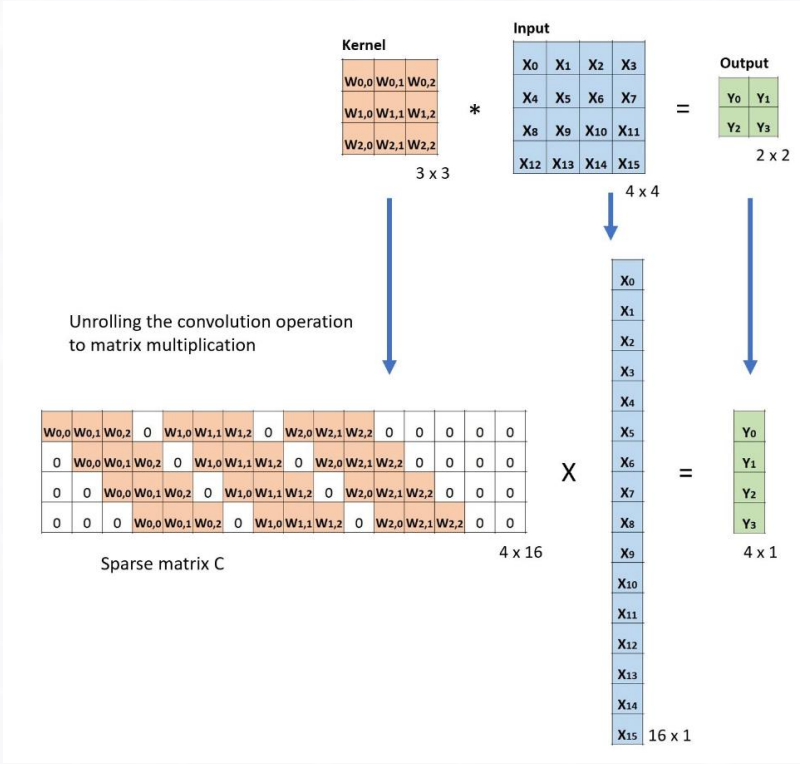


• In the example shown, we take a 4x4 input matrix and flatten it to 16x1; in addition, we transform the 3x3 kernel into a 4x16 **sparse, orthogonal matrix**. Using matrix multiplication, the resultant matrix is 4x1, which we then subsequently transform back to a 2x2 output.

# GAN: Transposed Convolution

• If, we multiply the equation **C x Large = Small**, by $C^T$, we arrive at: **$C^T$xSmall = Large**. In this way multiplication by the transposed convolution yields an up-sampling procedure. (for reference: we encountered this operation previously when discussing Aes and backpropagation through CNNs).

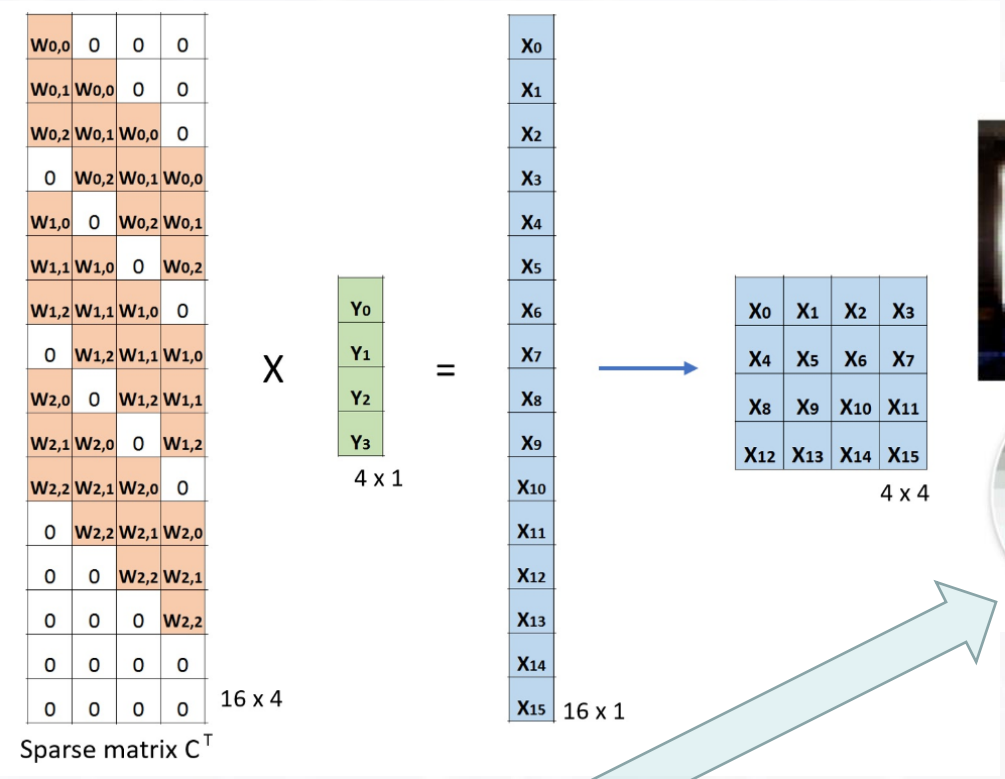


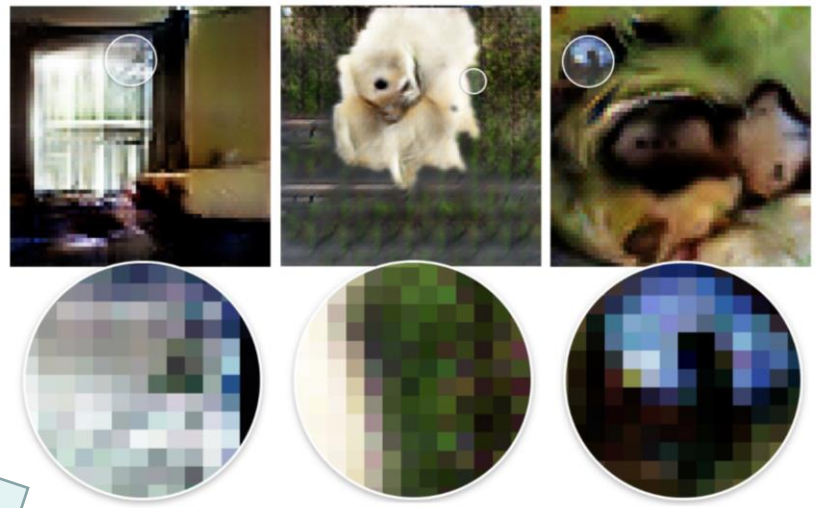

• Note that in practice, using a transposed convolution can lead to the presence of **checkerboard artifacts**; to alleviate this, practitioners commonly apply a two-step process instead: (i) bilinear up-sample, followed by (ii) convolution.

• For a comprehensive treatment of these topics, see: https://arxiv.org/abs/1603.07285

# GAN: Training

• In general, training the discriminator amounts to a supervised learning problem: we create a training set of (randomly inserted) real observations from the dataset interspersed with outputs produced by the generator (label 1 for true image, 0 for fakes). Recall that binary cross-entropy loss is defined:

$$L(y, p) = -\frac{1}{n}\sum_{i=1}^{n}\left(y_i \log(p_i) + (1-y_i)\log(1-p_i)\right)$$

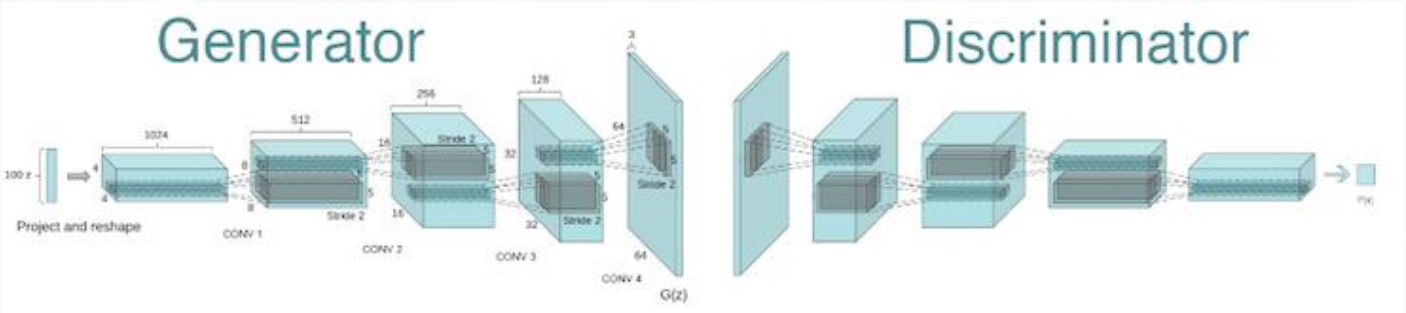

# GAN: Training

• In general, training the discriminator amounts to a supervised learning problem: we create a training set of (randomly inserted) real observations from the dataset interspersed with outputs produced by the generator (label 1 for true image, 0 for fakes). Recall that binary cross-entropy loss is defined:

$$L(y, p) = -\frac{1}{n}\sum_{i=1}^{n}\left(y_i \log(p_i) + (1-y_i)\log(1-p_i)\right)$$

• To train the GAN discriminator D, we calculate the loss when comparing predictions for real images $p_i = D(x_i)$ to the response $y_i = 1$ and predictions for generated images $p_i = D(G(z_i))$ to the response $y_i = 0$. Therefore, for the GAN discriminator, minimizing the loss function can be written as follows:

$$\min_D -\left(E_{x\sim p_X}\left[\log D(x)\right] + E_{z\sim p_Z}\left[\log\left(1-D(G(z))\right)\right]\right)$$

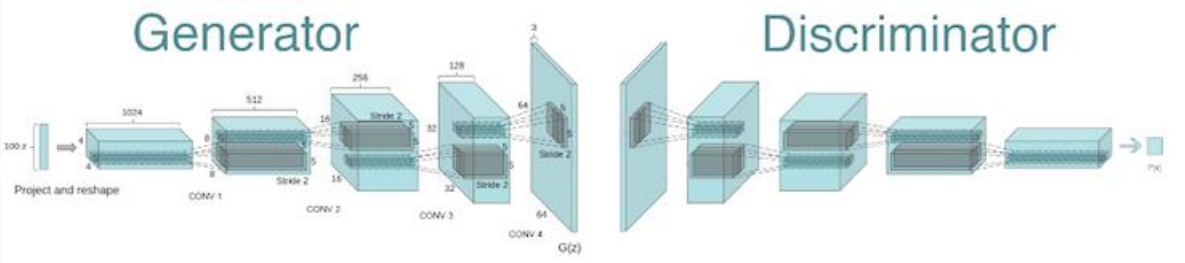

# GAN: Training

• **Training the generator is considerably more difficult**, as we don't readily have access to a training set that tells us the true image that a particular point in the latent space should be mapped to, for instance.

• To train the generator, we connect it to the discriminator by feeding the output from the generator into the discriminator so that the output from the combined model is the probability that a generated image is *real* (according to the discriminator).

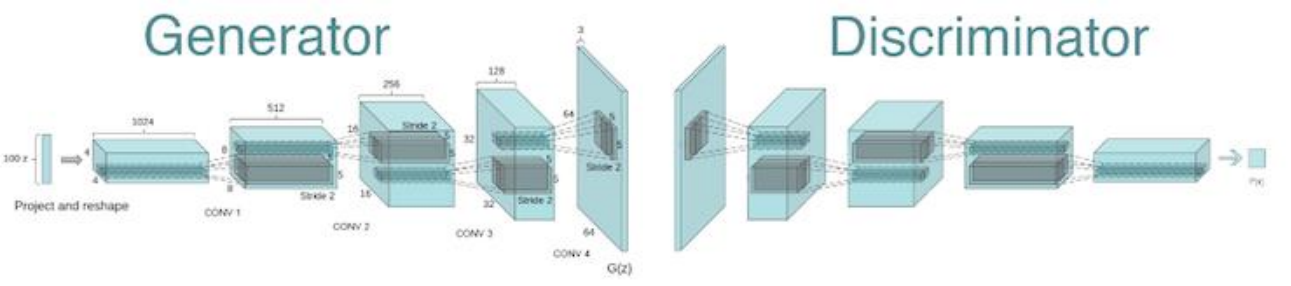

# GAN: Training

• We can train the combined model by creating training batches consisting of randomly generated latent vectors as input and a response which is set to 1, since we want to train the generator to produce images that the discriminator thinks are real. The loss is just binary cross-entropy loss between the output from the discriminator and the response vector of 1.

• Importantly, **we freeze the weights of the discriminator while we are training the combined model, so that only the generator's weights are updated**.

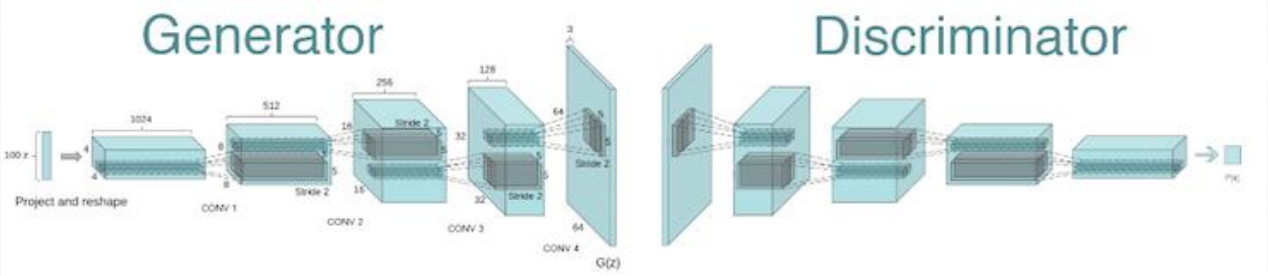

# GAN: Training

$$\min_D -\left(E_{x\sim p_X}\left[\log D(x)\right]+E_{z\sim p_Z}\left[\log\left(1-D(G(z))\right)\right]\right)$$

• To train the GAN generator G, we calculate the loss when comparing predictions for the generated images $p_i = D(G(z_i))$ to the response $y_i = 1$. Therefore, for the GAN generator, the minimizing loss function can be written as follows:

$$\min_G -\left(E_{z\sim p_Z}\left[\log\left(D(G(z))\right)\right]\right)$$

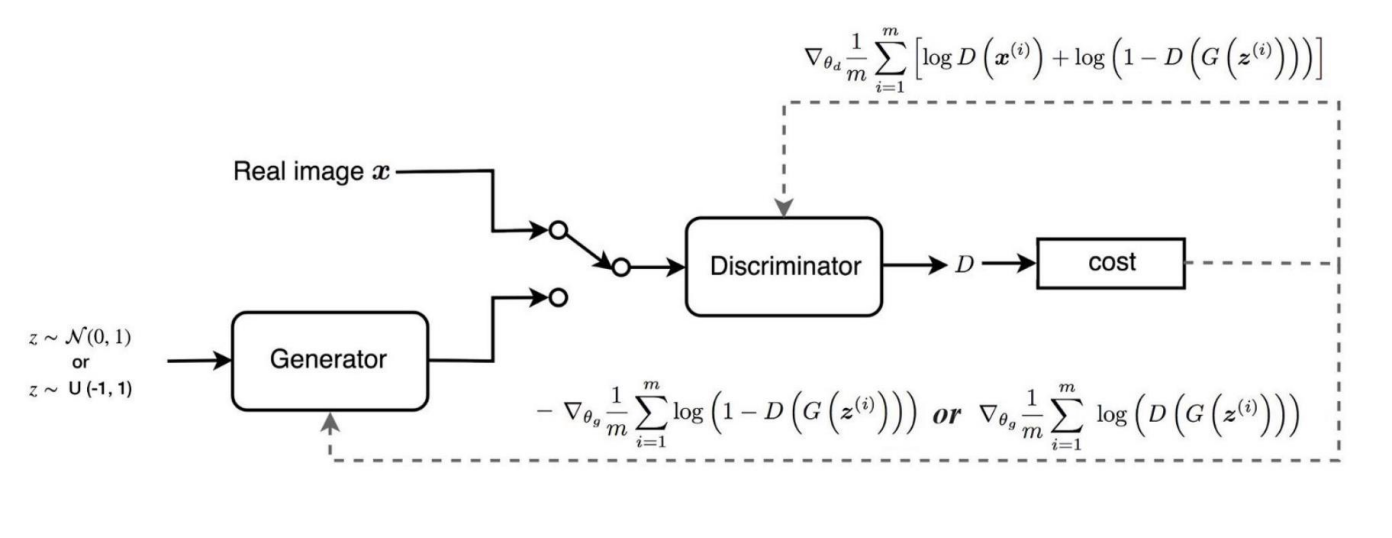

# GAN: Training

$$\min_D -\left(E_{x\sim p_X}\left[\log D(x)\right] + E_{z\sim p_Z}\left[\log\left(1 - D(G(z))\right)\right]\right)$$

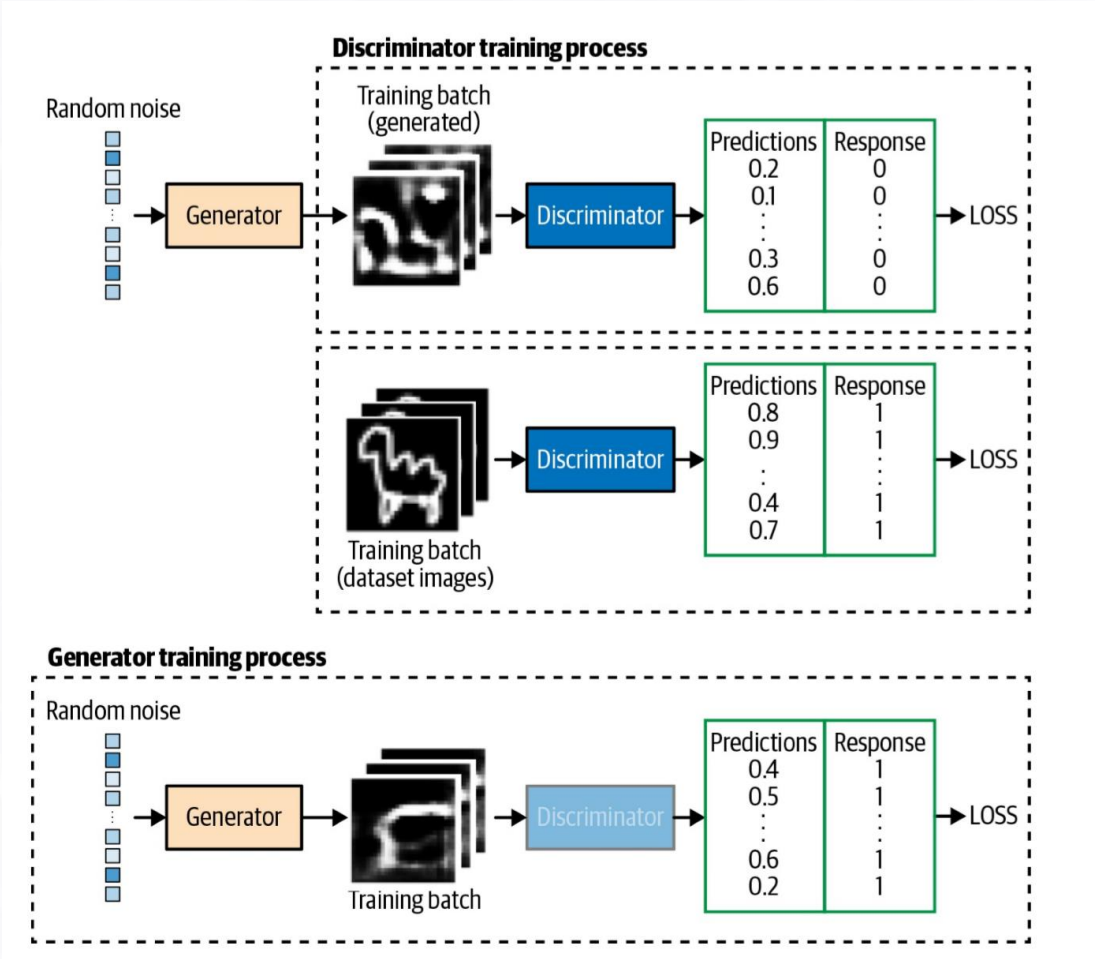


$$\min_G -\left(E_{z\sim p_Z}\left[\log\left(D(G(z))\right)\right]\right)$$

# GAN: Training

• GAN training is equivalent to a **zero-sum non-cooperative game**. From a game theory context, the GAN model converges when the discriminator and the generator reach a **Nash equilibrium**.

• If trained properly (which commonly requires the use of several "tricks" which we mention next), the discriminator and generator will converge to an equilibrium that allows the generator to learn meaningful information from the discriminator and the quality of the images will improve.

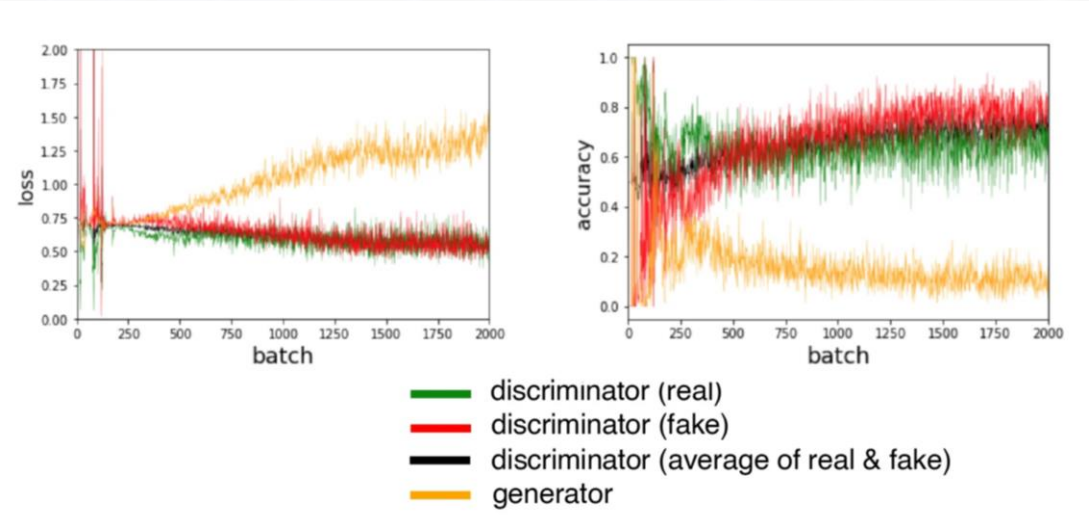


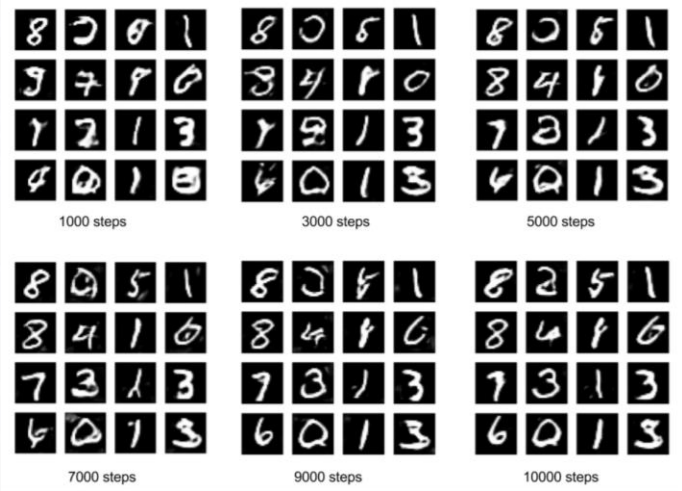

# GAN: Challenges

• GANs are notoriously difficult to train, for several reasons:

• **Mode Collapse**: Mode collapse occurs when the generator finds a small number of samples that fool the discriminator and therefore the generator isn't able to produce any examples other than this limited set.

• This can occur, say if we train the generator over several batches without updating the discriminator in between. In this situation, the generator would be inclined to find a singly observation that always fools the discriminator (the mode).

• **Oscillating Loss**: The losses of the discriminator and generator oscillate wildly. GANs are trained successfully when we observe a loss stabilization (shown in the previous slide); unfortunately, oscillating loss is common to vanilla GAN approaches.

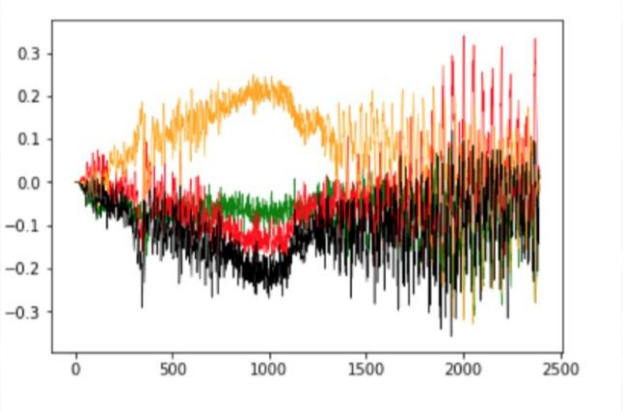

# GAN: CycleGAN

**Unpaired Image-to-Image Translation using Cycle-Consistent Adversarial Networks**

Jun-Yan Zhu* Taesung Park* Phillip Isola Alexei A. Efros
Berkeley AI Research (BAIR) laboratory, UC Berkeley

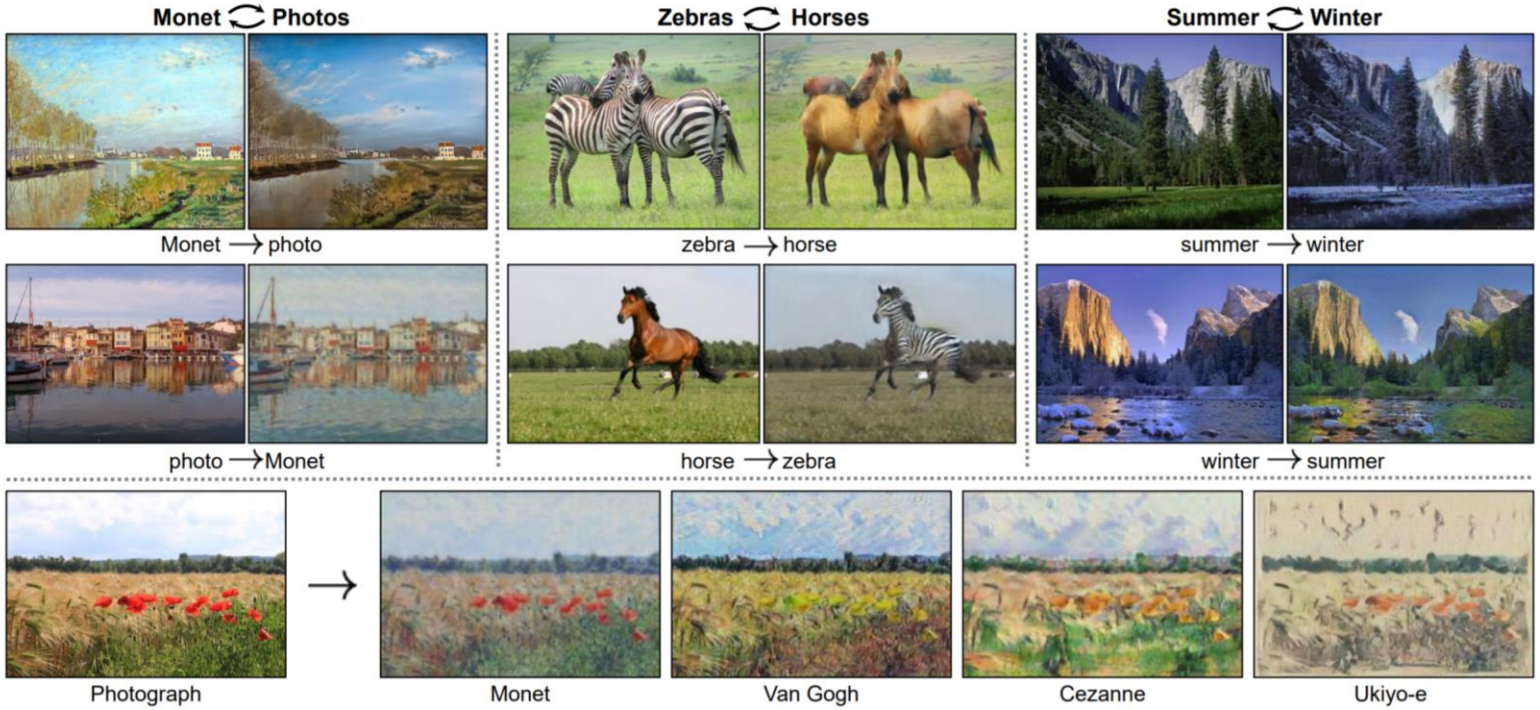


Figure 1: Given any two unordered image collections $X$ and $Y$, our algorithm learns to automatically "translate" an image

https://arxiv.org/pdf/1703.10593.pdf

# GAN: CycleGAN

• For the image translation task, CycleGAN trains without using paired examples.

• CycleGAN is composed of (4) sub-models: two generators and two discriminators. The first generator $G_{AB}$ converts images from domain A to domain B; whereas the second generator $G_{BA}$, converts images from domain B to domain A.

• The authors employ a **U-Net architecture** (shown on the right) for the generator models.

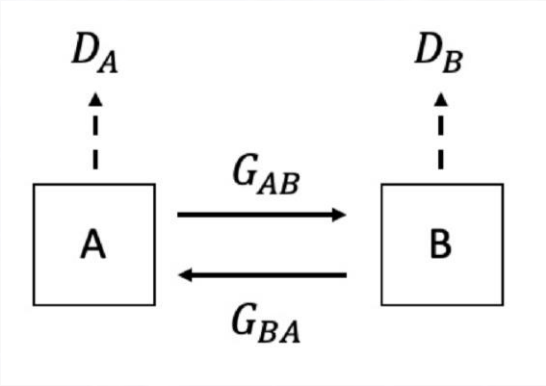


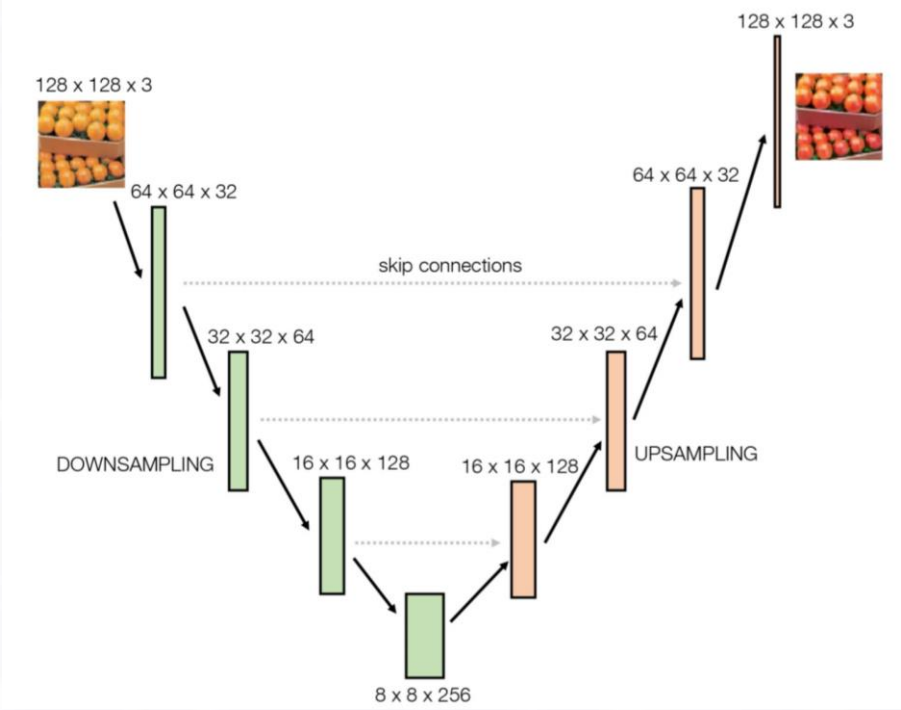

# "World Models" GAN

• Ha and Schmidhuber (NeurIPS, 2018) presented "World Models"*, a paradigm for training RL agents using a VAE, whereby an agent is trained:

"**entirely insides of its own hallucinated dream generated by its world model, and [we] transfer this policy back into the actual environment.**"

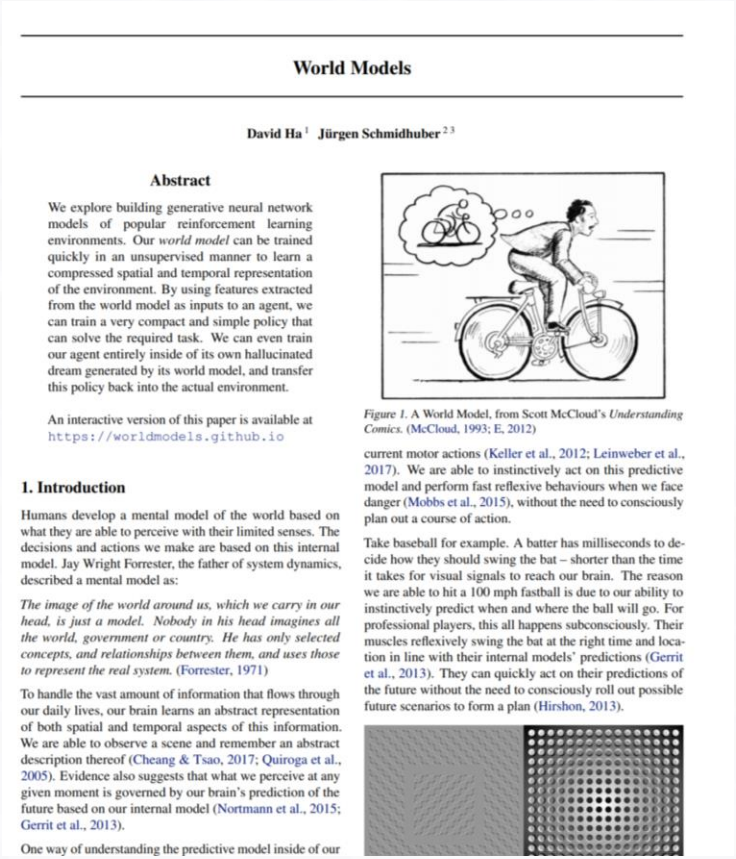

**World Models**

David Ha [1] Jürgen Schmidhuber [2 3]

**Abstract**

We explore building generative neural network models of popular reinforcement learning environments. Our *world model* can be trained quickly in an unsupervised manner to learn a compressed spatial and temporal representation of the environment. By using features extracted from the world model as inputs to an agent, we can train a very compact and simple policy that can solve the required task. We can even train our agent entirely inside of its own hallucinated dream generated by its world model, and transfer this policy back into the actual environment.

An interactive version of this paper is available at https://worldmodels.github.io

**1. Introduction**

Humans develop a mental model of the world based on what they are able to perceive with their limited senses. The decisions and actions we make are based on this internal model. Jay Wright Forrester, the father of system dynamics, described a mental model as:

*The image of the world around us, which we carry in our head, is just a model. Nobody in his head imagines all the world, government or country. He has only selected concepts, and relationships between them, and uses those to represent the real system.* (Forrester, 1971)

To handle the vast amount of information that flows through our daily lives, our brain learns an abstract representation of both spatial and temporal aspects of this information. We are able to observe a scene and remember an abstract description thereof (Cheang & Tsao, 2017; Quiroga et al., 2005). Evidence also suggests that what we perceive at any given moment is governed by our brain's prediction of the future based on our internal model (Nortmann et al., 2015; Gerrit et al., 2013).

One way of understanding the predictive model inside of our



*Figure 1.* A World Model, from Scott McCloud's *Understanding Comics.* (McCloud, 1993; E, 2012)

current motor actions (Keller et al., 2012; Leinweber et al., 2017). We are able to instinctively act on this predictive model and perform fast reflexive behaviours when we face danger (Mobbs et al., 2015), without the need to consciously plan out a course of action.

Take baseball for example. A batter has milliseconds to decide how they should swing the bat – shorter than the time it takes for visual signals to reach our brain. The reason we are able to hit a 100 mph fastball is due to our ability to instinctively predict when and where the ball will go. For professional players, this all happens subconsciously. Their muscles reflexively swing the bat at the right time and location in line with their internal models' predictions (Gerrit et al., 2013). They can quickly act on their predictions of the future without the need to consciously roll out possible future scenarios to form a plan (Hirshon, 2013).



*https://worldmodels.github.io/

*https://arxiv.org/pdf/1803.10122.pdf

# "World Models" GAN

The pipeline consists of (3) fundamental components:

(1) The **Vision Model** (**V**), A VAE that encodes high-dimensional observations into a low-dimensional latent vector.

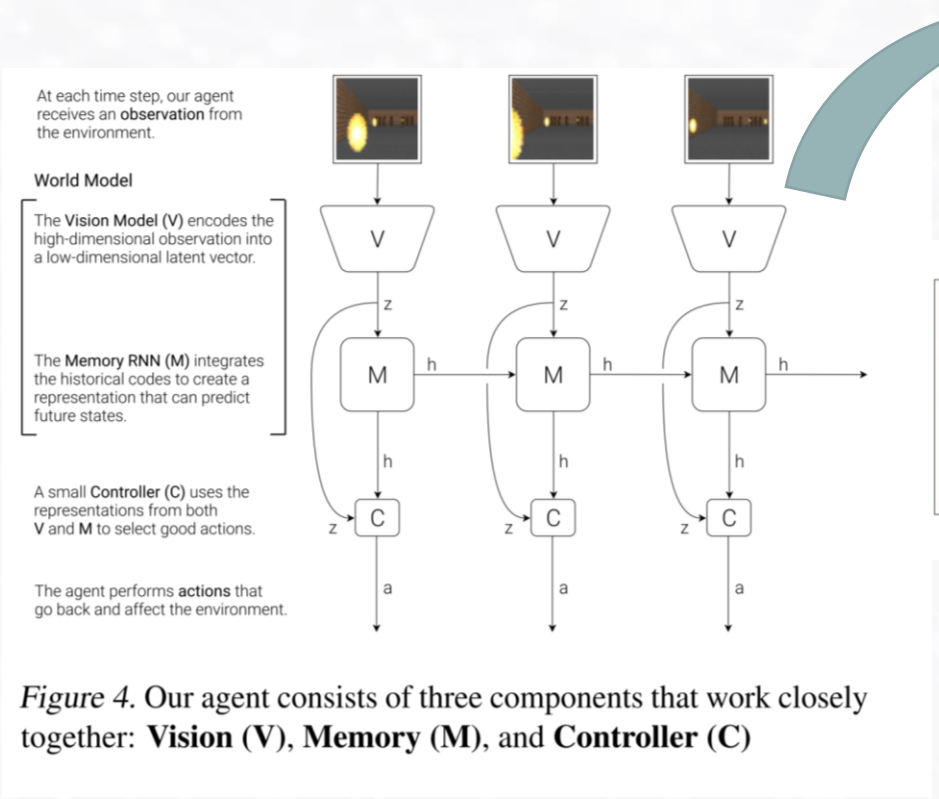


*Figure 4.* Our agent consists of three components that work closely together: **Vision (V)**, **Memory (M)**, and **Controller (C)**

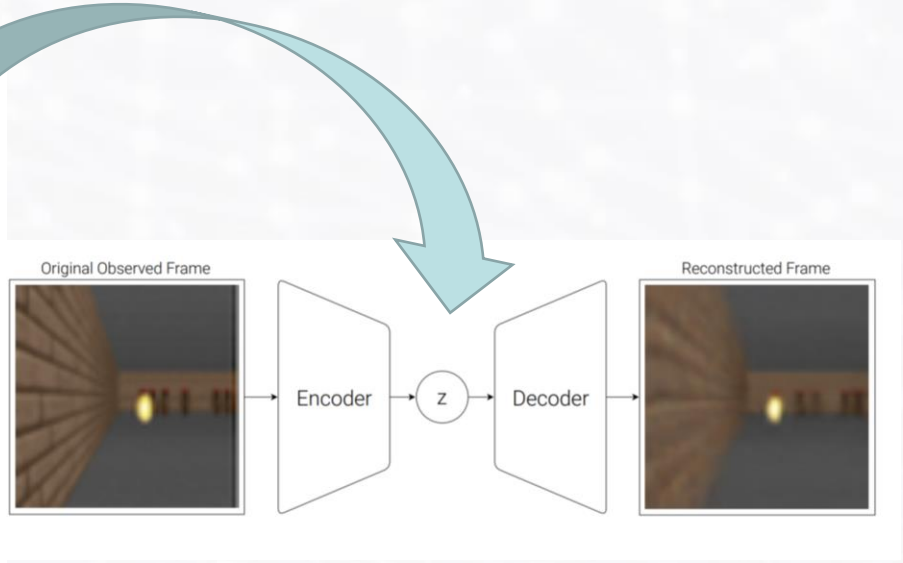

# "World Models" GAN

The pipeline consists of (3) fundamental components:

(2) A **Memory RNN** (**M**): this unit approximates $p(z_t)$ using a GMM (Gaussian Mixture Model); the RNN is trained to output the probability distribution of the next latent vector $z_{t+1}$ given the current and past information available to it -- specifically predict: $p(z_{t+1}|a_t, z_t, h_t)$

• Technically, $M$ incorporates a **Mixture Density Network** (MDN), which has been used previously for "sequence generation" (e.g., handwriting, as shown below left).

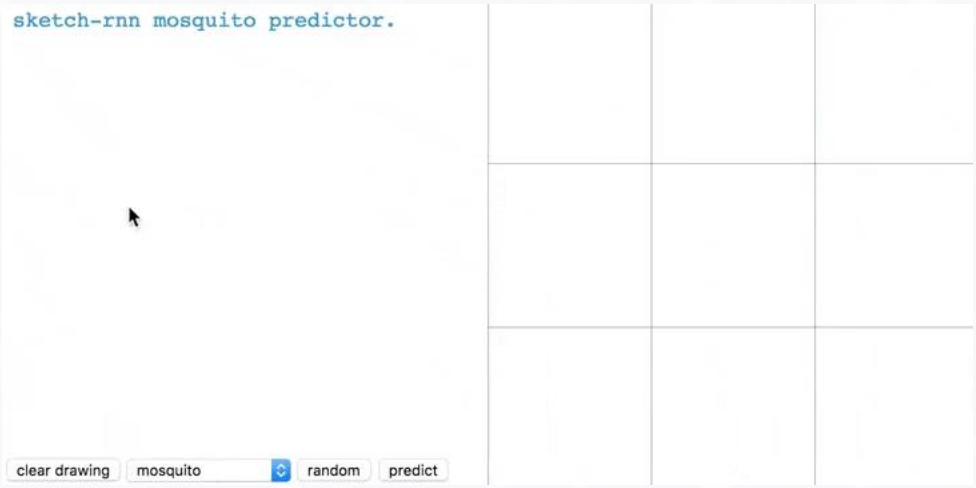


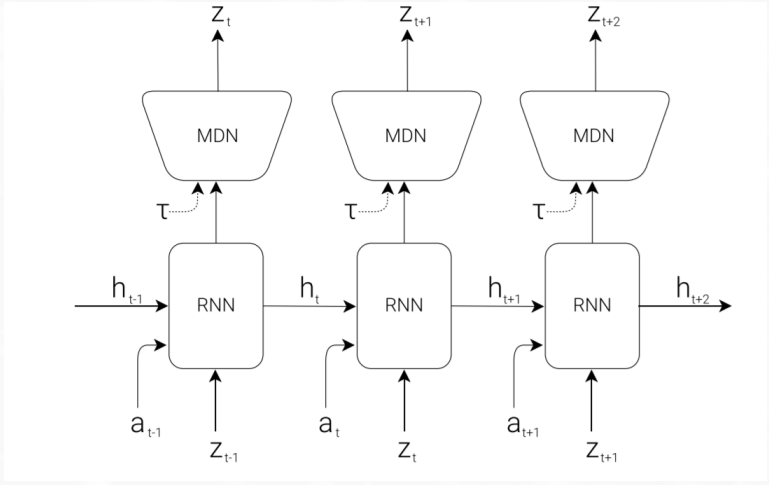

# "World Models" GAN

The pipeline consists of (3) fundamental components:

(3) A **controller** (**C**) (a simple, ~1k parameters) RL agent that determines the course of actions to take in order to maximize the expected cumulative reward of the agent during a rollout of the environment.

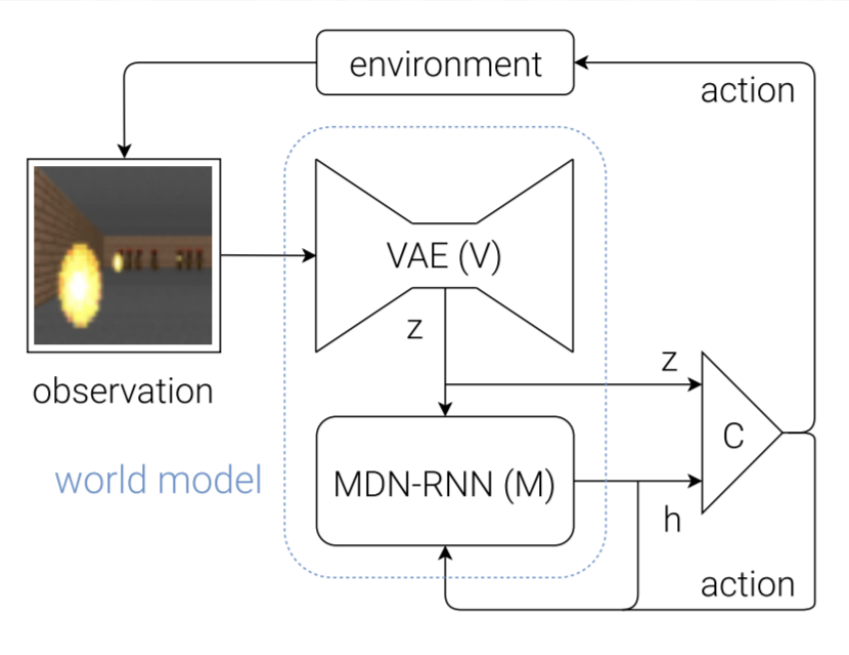


| Model | Parameter Count |
|---|---|
| VAE | 4,446,915 |
| MDN-RNN | 1,678,785 |
| Controller | 1,088 |

In summary: (1) VAE learns a latent mapping of images to $z_t$;
(2) the MDN-RNN module produces the next frame hidden context and next frame "dream" latent vector $z_{t+1}$;
(3) the controller C executes the roll-out simulation in the "dream-world."

# "World Models" GAN

Training with simulated dreams!

• Because the model can predict the future (!), the authors can use it to generate hypothetical racing scenarios on its own. They produce the probability distribution of the latent variable, given the current states, and sample a $z_{t+1}$ in place of a real observation. The controller acts in the hallucinated environment generated by M.

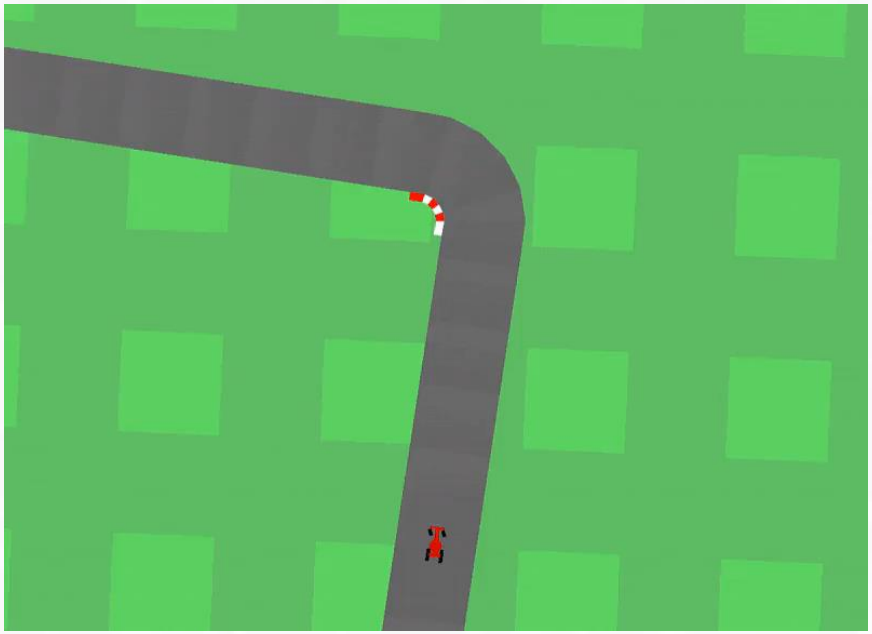

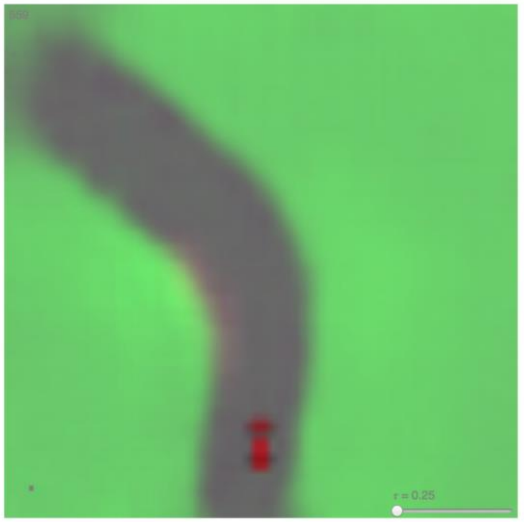

*Figure 13.* Our agent driving inside of its own dream world. Here, we deploy our trained policy into a fake environment generated by the MDN-RNN, and rendered using the VAE's decoder. In the demo, one can override the agent's actions as well as adjust $\tau$ to control the uncertainty of the environment generated by M.

# “World Models” GAN

VizDoom from World Models.

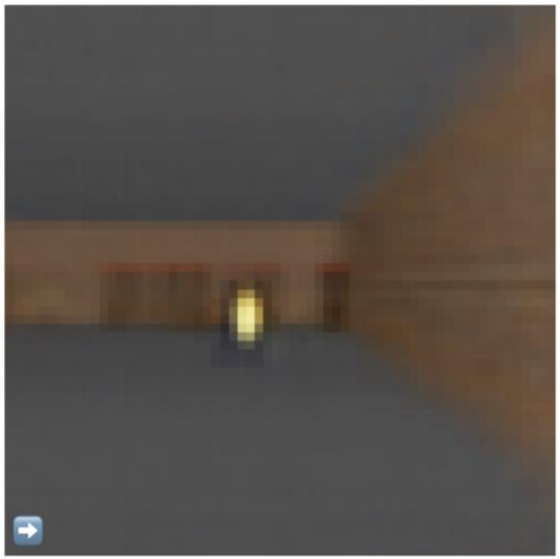

*Figure 15.* Our agent discovers a policy to avoid hallucinated fireballs. In the online version of this article, the reader can interact with the environment inside this demo.

# GAMEGAN

• In 2014 Minh et al., (Deepmind) published the seminal research "Playing Atari with Deep Reinforcement Learning."*

• This work leveraged DL and RL together to produce a generalizable algorithm with "superhuman" performance on Atari games. Remarkably, this model was trained strictly through self-play (i.e., the agent has no prior knowledge or information about the game engine/logic).

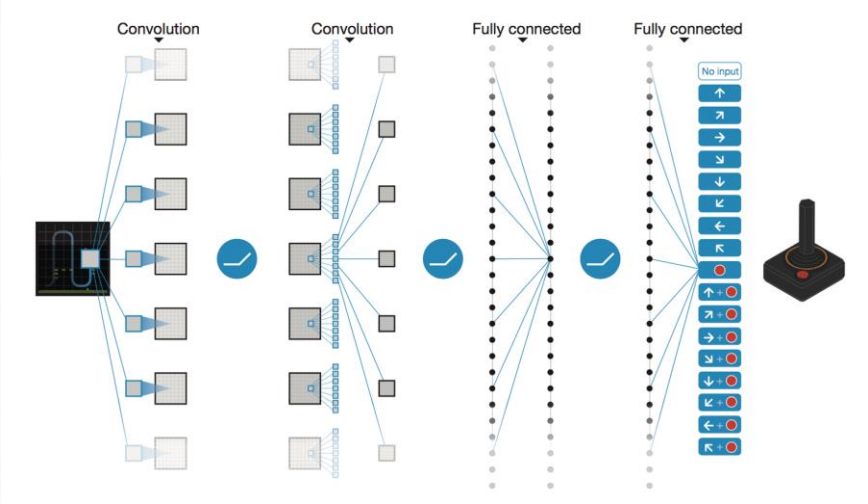


*https://www.cs.toronto.edu/~vmnih/docs/dqn.pdf
*RL and the Atari paper are covered in depth in my 4/541 course.

# GAMEGAN

• Kim et al. published the outstanding work "Learning to Simulate Dynamic Environments with GameGAN"* (2020), an algorithm that learns to generate an underlying game engine(!) from observations of gameplay (including user inputs) – the model is not given access to any underlying game logic or the actual game engine at any time.

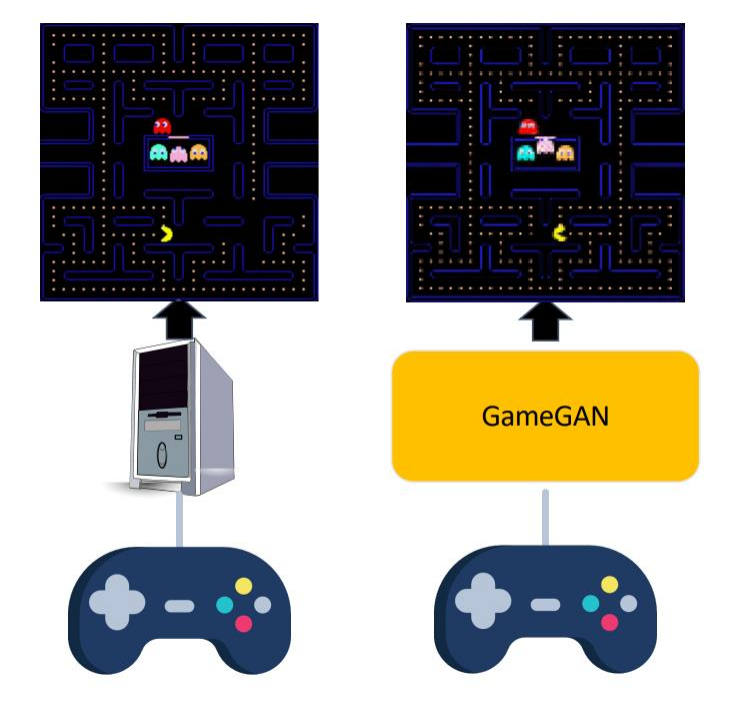


*https://arxiv.org/pdf/2005.12126.pdf

# GAMEGAN

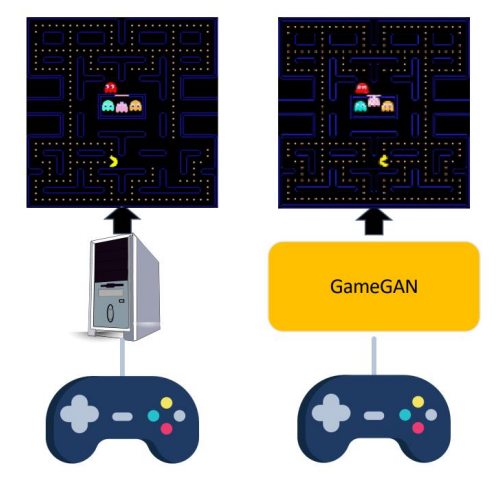


• While the domain of this research focuses on game-playing, the larger motivation behind this research is to push the state-of-the-art to **improve the fidelity of complex simulations**, and to show that the dynamics of these environments can be learned effectively, and indirectly by leveraging ML.

• Complex simulations are essential to many branches of science, including the medical sciences, particularly drug efficacy studies, robotics, automation, engineering, physics, chemistry, etc. The authors argue that learning to simulate by simply observing is the most scalable way going forward.

*https://arxiv.org/pdf/2005.12126.pdf

# GAMEGAN

• *GAMEGAN* uses an action-conditioned (conditioned on the key pressed by an agent) GAN to predict the next frame of a game. This research is similar to GAN-based video prediction models which predict future frames, however an extra challenge for this problem setting is the presence of stochasticity in the environment (e.g., ghost movements in Pac-man).

• To this end, GAMEGAN not only predicts the next frame of the game, but it must also learn the intrinsic dynamics of the environment.

# GAMEGAN

• The authors introduce several key innovations in their workflow, including a memory module to better capture long-term prediction consistency, and a carefully-designed decoder that disentangles static and dynamic components of the game (e.g., maze elements vs. ghosts).

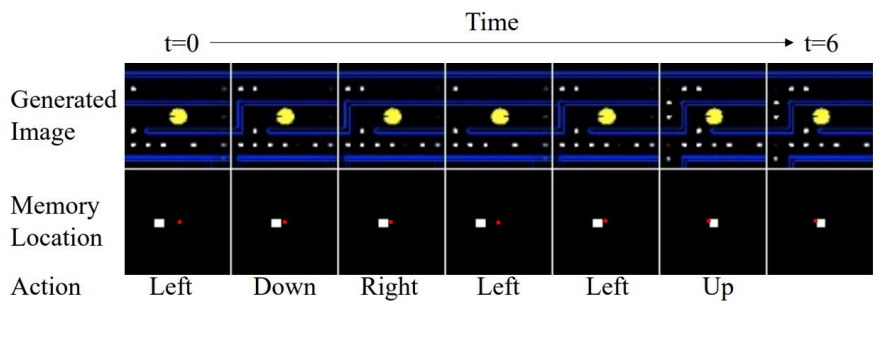


Visualizing memory module: location of egocentric agent is tracked with attention; notice maze generation is consistent when return to location at t=0.

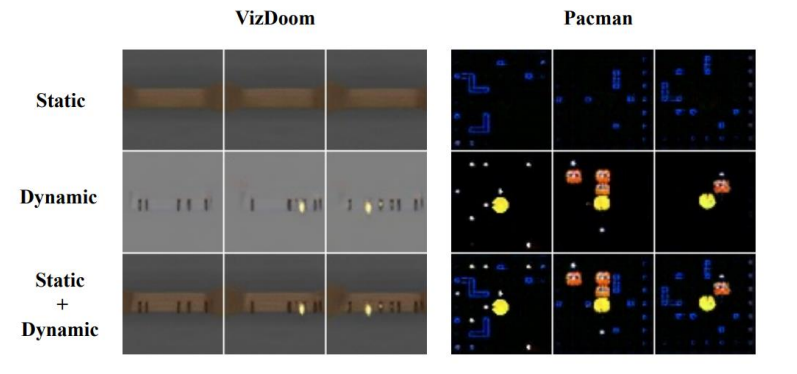


Decoder disentangles static and dynamic components of game.

# GAMEGAN

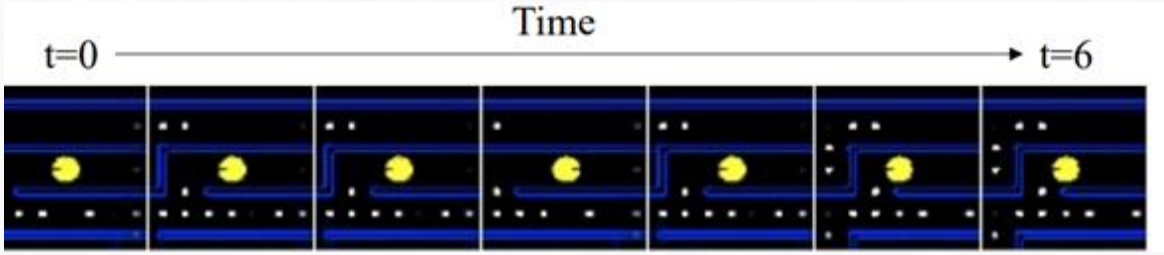


• *GAMEGAN* focuses on **action-conditioned simulation** in the image space with an egocentric agent that moves according to the given action $a_t \sim A$ at a time $t$ and generates a new observation/state $x_{t+1}$.

• The authors assume there is also a stochastic variable $z_t \sim N(0, I)$ that corresponds with randomness in the environment. Given the history of images $x_{1:t}$, along with $a_t$ and $z_t$, GameGAN predicts the next image $x_{t+1}$.

# GAMEGAN

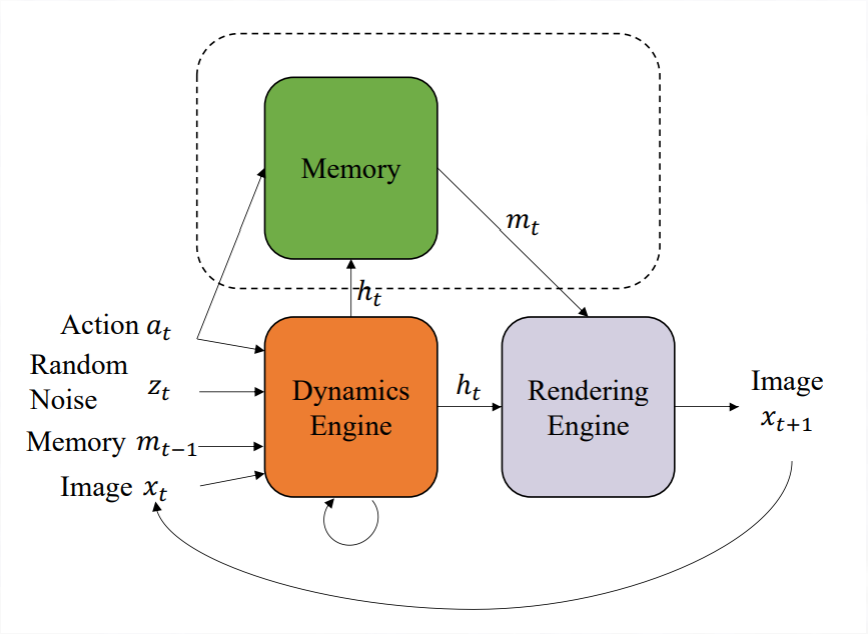


- In total, GAMEGAN consists of three key components:

**(1) Dynamics Engine:** learns "licit" environment transitions (e.g., Pac-Man can't move through a wall, etc.) using an **action-conditioned LSTM**. As with a standard LSTM, this module maintains both $h_t$ hidden representation and $c_t$ context parameters, in addition to processing action and stochastic variables.

# GAMEGAN

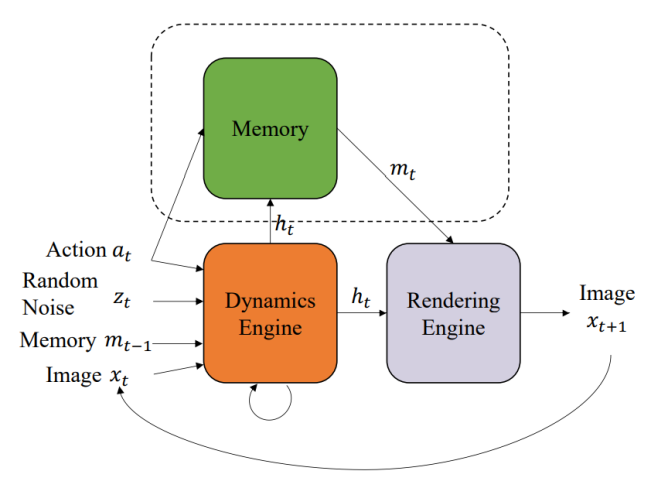


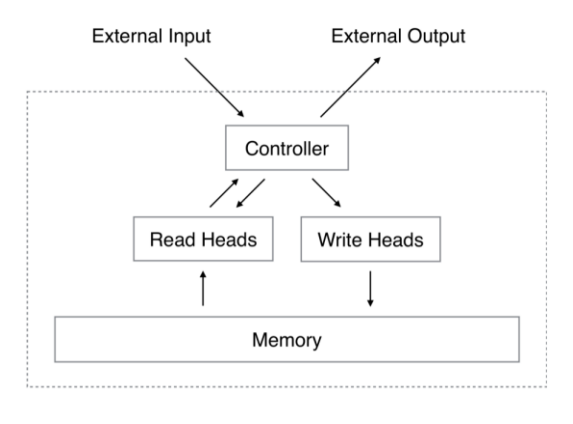


• In total, GAMEGAN consists of three key components:

**(2) Memory Module**: maintains long-term consistency of static elements (e.g., maze). Challenges for conventional RNNs include: (i) need to remember every scene it generates, and (ii) design a loss function that enforces such long-term consistency.

• Motivated by **Neural Turing Machines*** (NTM), the memory module has a memory block and attended location at time $t$ (denoted $\alpha_t$). One can think of the memory block as corresponding with the location of the egocentric agent and $\alpha_t$ corresponds with the current location. Enforcing long-term consistency amounts to remembering generated static elements.

*https://arxiv.org/pdf/1410.5401.pdf

# GAMEGAN

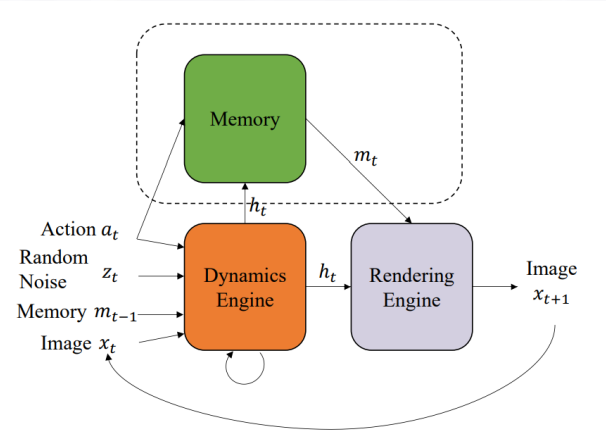


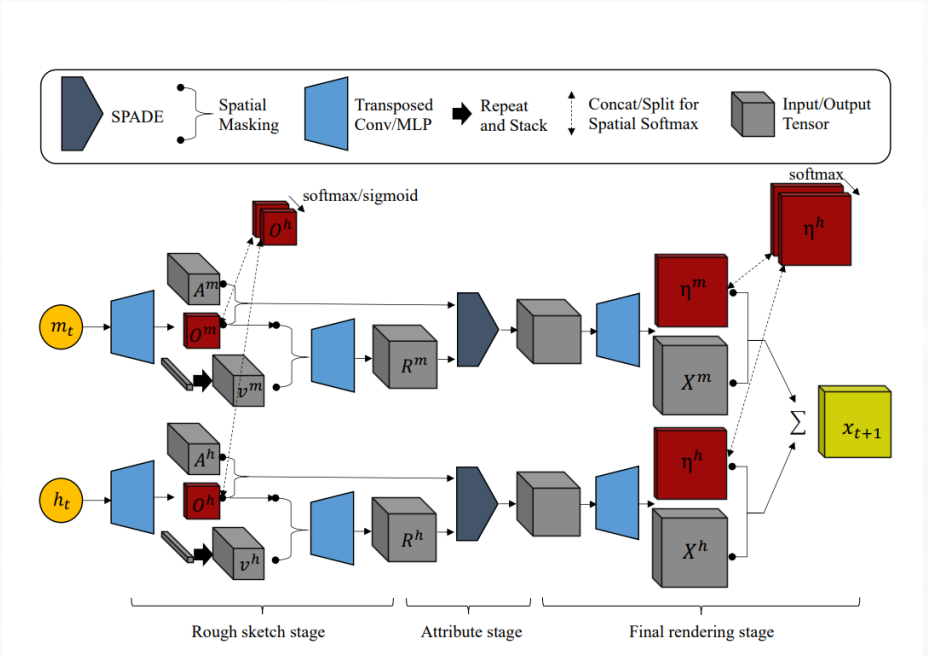


- In total, GAMEGAN consists of three key components:

**(3) Rendering engine**: responsible for rendering simulated image $x_{t+1}$, given the internal state $h_t$ (from dynamics engine, LSTM). The authors introduce a specialized rendering architecture to ensure long-term consistency by learning to produce disentangled scenes.

# GAMEGAN

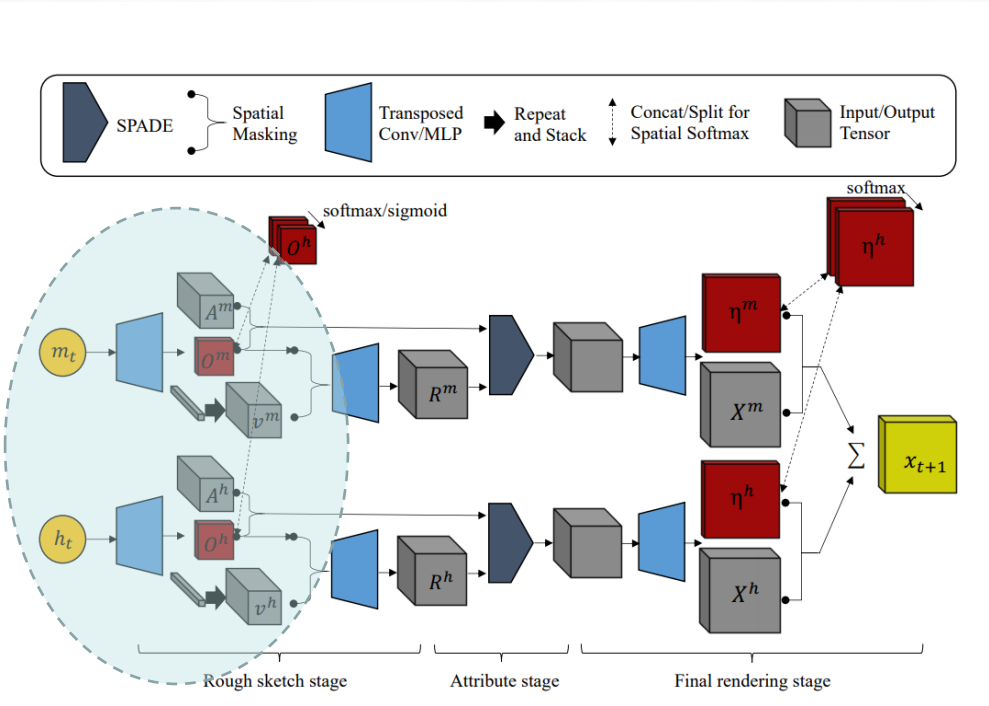


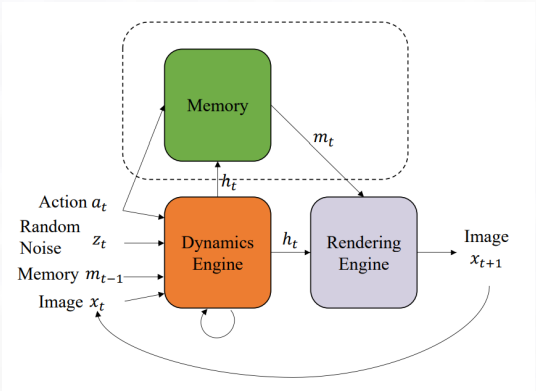


**(3) Rendering engine** (RE): responsible for rendering simulated image $x_{t+1}$, given the internal state $h_t$ (from dynamics engine, LSTM). The authors introduce a specialized rendering architecture to ensure long-term consistency by learning to produce disentangled scenes.

• The RE takes as input $h_t$ (from LSTM) and $m_t$ from the memory module. In the first step the RE applies a CNN, outputting an **attribute map** $A^m$ and **object map** $O^m$; the inputs ($h_t$ and $m_t$ ) are also fed into linear layer to get a **type vector**, denoted $v^m$.

# GAMEGAN

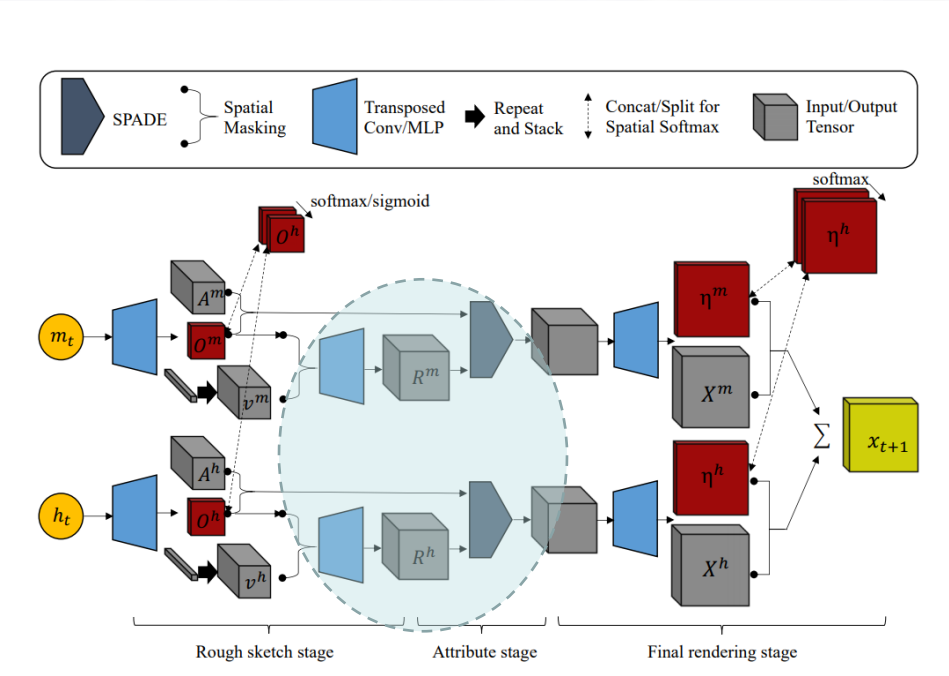


**(3) Rendering engine** (RE): responsible for rendering simulated image $x_{t+1}$, given the internal state $h_t$ (from dynamics engine, LSTM). The authors introduce a specialized rendering architecture to ensure long-term consistency by learning to produce disentangled scenes.

• $O^m$ and $v^m$ are concatenated and fed into an additional conv net, producing $R^m$ the rough sketch of where each object is located.

# GAMEGAN

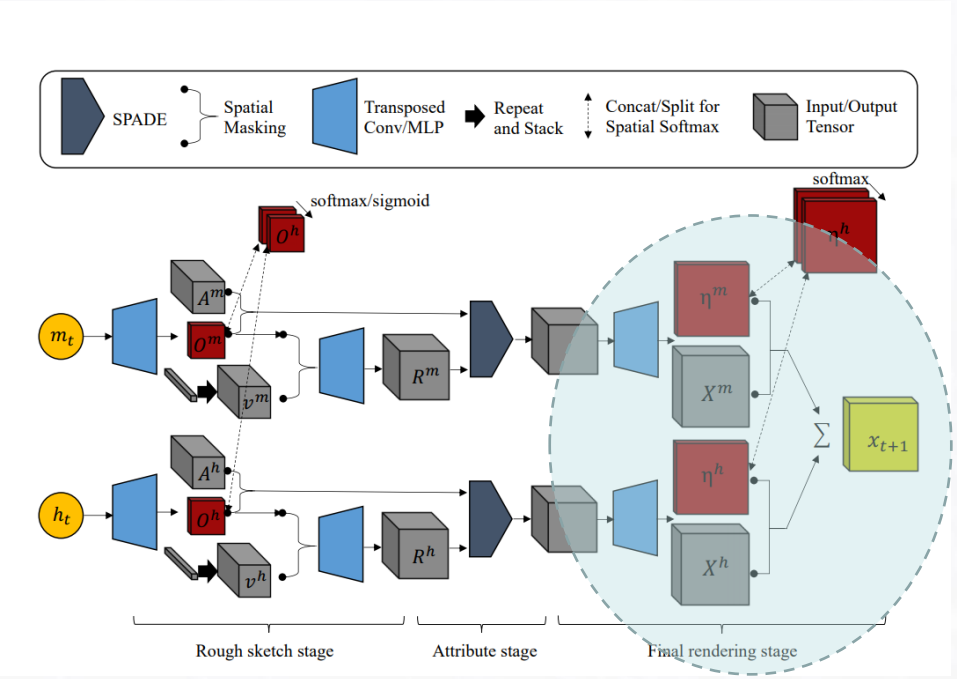


**(3) Rendering engine** (RE): responsible for rendering simulated image $x_{t+1}$, given the internal state $h_t$ (from dynamics engine, LSTM). The authors introduce a specialized rendering architecture to ensure long-term consistency by learning to produce disentangled scenes.

• The location is insufficient alone to render an accurate simulation, as attributes (e.g., color of ghost) must also be accounted for. The attribute map $A^k$ is elementwise multiplied by the rough location tensor $R^k$ , then fed through a transposed convolution, which renders a fine mask $\eta^k$ that accounts for the "depth" of objects (to handle occlusions such as Pac-Man intersecting a ghost). The final output is the predicted state $x_{t+1}$.

# GAMEGAN

Finally, the model is trained using three adversarial loss components:

**(1) Single image discriminator**: to ensure each generated frame is realistic, the discriminator and GameGAN simulator play an adversarial game.

**(2) Action-conditioned discriminator**: GameGAN needs to reflect the actions taken by the agent faithfully, this loss reflects predicted image *and* action provided by the agent.

**(3) Temporal discriminator**: Using a 3D convolution network, the authors employ a temporal discriminator to decide whether a sequence of frames is real or fake.

The authors also introduce a **cycle loss** function that encourages the model to keep static elements in memory.

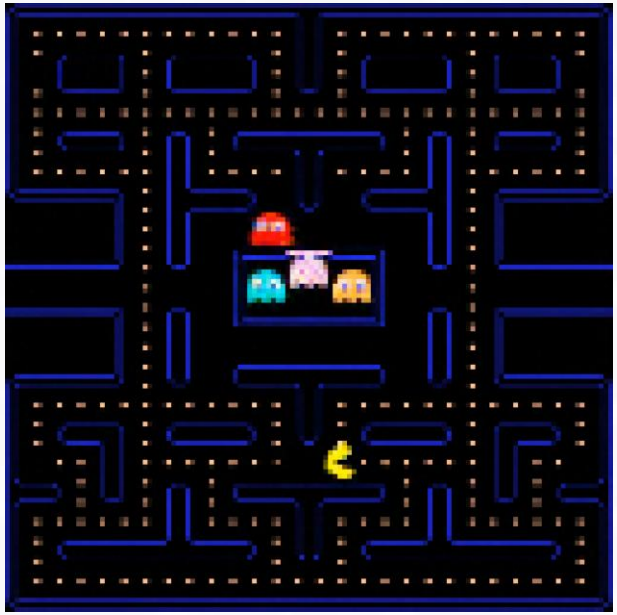

https://nv-tlabs.github.io/gameGAN/

# Graph Neural Networks

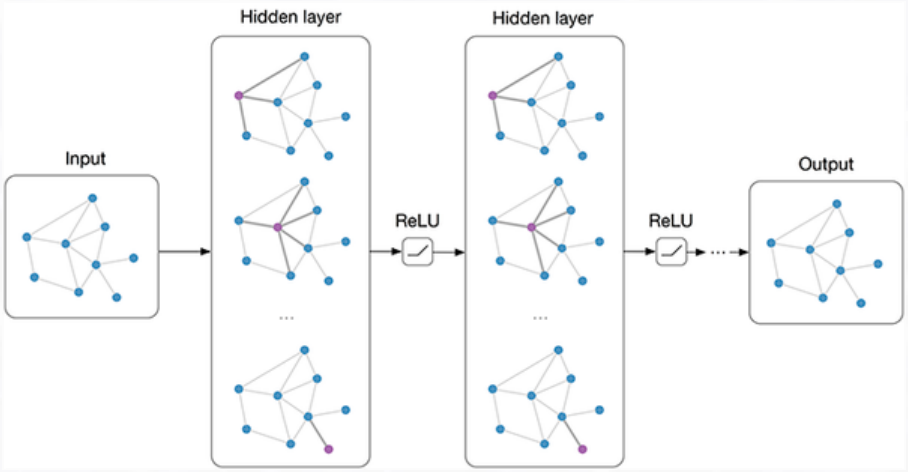


"Graphs are the most important discrete models in the world" G. Strang (MIT)

• Graph data can denote a very large sets of diverse systems: molecules, social networks, images, etc.

• GNNs are a burgeoning DL-based method operating on graphs.

• Many classic DL models (e.g., CNN, RNN, LSTM, attention models, etc.) have been "ported" to the GNN framework; GNNs can encompass classification, regression prediction, segmentation, etc., tasks.

•Why use GNNs? (1) Natural fit for graph data; (2) GNNs can learn *anisotropic filters* (for CV tasks).

https://arxiv.org/pdf/1901.00596.pdf

# Graph Neural Networks

Basics of GNNs

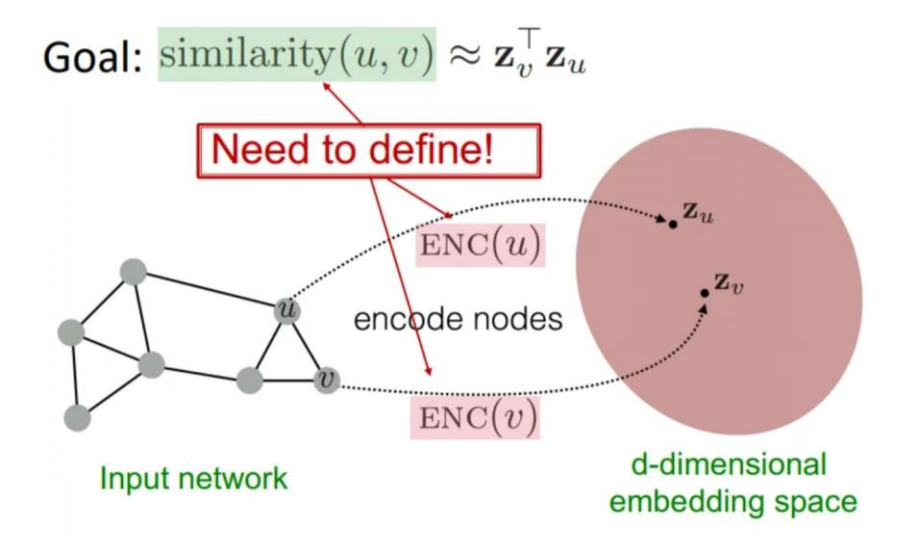


• For GNNs, we have a global graph structure; in addition, each node has an associated *feature vector* (e.g., encoding of atom in a molecule, RGB values in image, etc.). Just like with standard NNs, GNNs learn an embedding – a **node embedding**.

• GNNs perform forward propagation through "**message-passing**", e.g., aggregating local information and then performing a DNN-type computation, such as a linear transformation followed by a non-linear operation.

# Graph Neural Networks

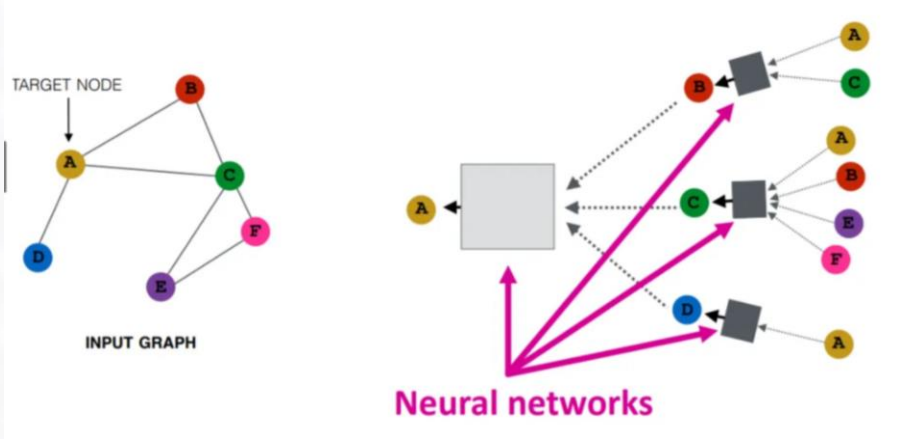


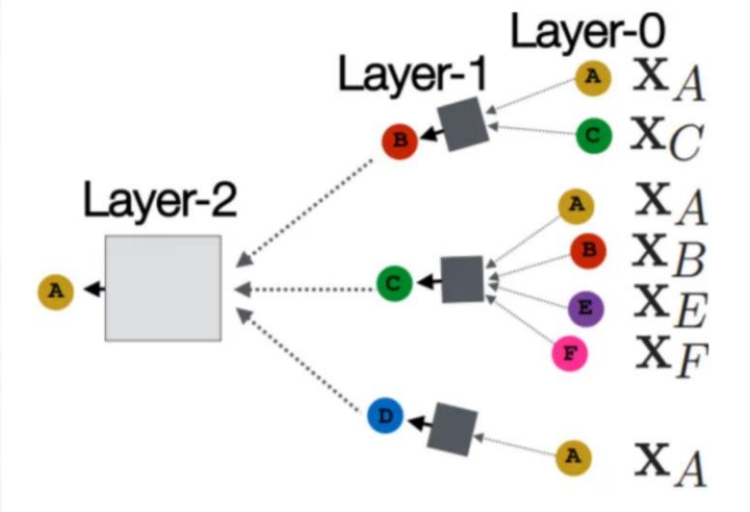


$$h_v^k = \sigma(W_k \sum \frac{h_u^{k-1}}{\mid N(v)} + B_k h_v^{k-1}) \text{ where } k = 1, ..., k-1$$

• **Aggregation** typically involves some basic operation on the neighbors of a target node (e.g., mean or sample mean of neighbors). Aggregation preserves local information in the graph.

• Typically, a single linear layer NN is used to propagate updates to nodes from one-step neighbors.

• This "unrolling" process continues for two-step neighbors, and so on. The parameters of the GNN are comprised of the weights used in the message-passing process.

# Graph Neural Networks

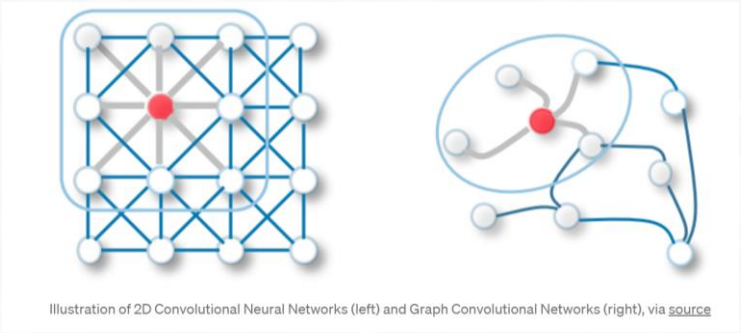

Illustration of 2D Convolutional Neural Networks (left) and Graph Convolutional Networks (right), via source

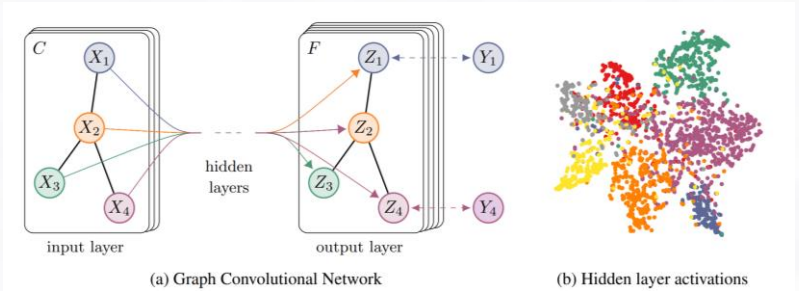


Figure 1: *Left*: Schematic depiction of multi-layer Graph Convolutional Network (GCN) for semi-supervised learning with $C$ input channels and $F$ feature maps in the output layer. The graph structure (edges shown as black lines) is shared over layers, labels are denoted by $Y_i$. *Right*: t-SNE (Maaten & Hinton, 2008) visualization of hidden layer activations of a two-layer GCN trained on the Cora dataset (Sen et al., 2008) using 5% of labels. Colors denote document class.

• Unlike classical CNNs, GCNs can learn **anisotropic filters**. Notice that "convolution" does not necessarily entail image processing. Instead, one can think of label information over a graph as being "smoothed" over the graph.

• In the original GCN* (Kipf, et al.) paper, propagation is defined using the normalized graph Laplacian:

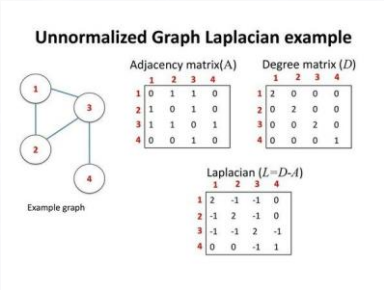


$$H^{(l+1)} = \sigma\left(\tilde{D}^{-\frac{1}{2}}\tilde{A}\tilde{D}^{-\frac{1}{2}}H^{(l)}W^{(l)}\right)$$

*https://arxiv.org/pdf/1609.02907.pdf

*Fin*